LiDAR-based pallet condition evaluation in automated Storage and Retrieval Machines

Francisco Manuel Gomes Queirós

Masters Dissertation

FEUP Supervisor: Prof. António José Pessoa de Magalhães

Körber Supply Chain PT Supervisor: Eng. João Gonçalves Costa

U. PORTO

FEUP FACULDADE DE ENGENHARIA
UNIVERSIDADE DO PORTO

Masters Degree in Mechanical Engineering

Automation Branch

July 2025

LiDAR-based pallet condition evaluation in automated Storage and Retrieval Machines

Abstract

In the context of increasingly automated warehouse operations, the reliability and precision of material handling systems play a critical role in ensuring efficiency and safety. This dissertation presents the development of a technological solution designed to enhance the performance of Storage and Retrieval Machines (SRMs) by enabling the real-time evaluation of pallet conditions. The proposed system integrates a SICK multiScan LiDAR (Light Detection and Ranging) sensor with a Siemens S7-1200 PLC (Programmable Logic Controller) to detect and correct positional misalignments between the SRM and the pallet, such as horizontal, vertical, and rotational offsets, as well as to identify structural faults that may lead to collisions or load drops.

The project includes the definition of technical requirements, the integration and configuration of the LiDAR sensor, the development of a detection algorithm, and the implementation of real-time data acquisition and processing within the PLC. Experimental tests were conducted to validate the system's performance under realistic conditions. The results demonstrated promising accuracy in estimating horizontal and rotational deviations, while also highlighting limitations in detecting vertical offsets and structural faults due to mechanical tolerances and sensor resolution.

Overall, the proposed solution contributes to increasing the reliability and safety of SRM operations, particularly in high-density automated warehouses, and establishes a foundation for future improvements involving higher-resolution sensing and adaptive algorithms.

Keywords: LiDAR, PLC, SRM, Automated Warehouses

LiDAR-based pallet condition evaluation in automated Storage and Retrieval Machines

Resumo

No contexto do aumento das operações de armazéns automáticos, a fiabilidade e a precisão dos sistemas de movimentação de materiais assumem um papel crítico e essencial para garantir a eficiência e a segurança. Esta dissertação apresenta o desenvolvimento de uma solução tecnológica concebida para melhorar o desempenho dos transelevadores (SRMs), através da avaliação em tempo real das condições das paletes a serem carregadas. A solução proposta integra um sensor LiDAR (Light Detection and Ranging) (multiScan165 da SICK) com um autómato programável Siemens S7-1200 (PLC), permitindo estimar e corrigir desalinhamentos posicionais entre o SRM e a palete, tais como desvios horizontais, verticais e rotacionais, assim como identificar falhas estruturais que possam conduzir a colisões ou quedas de carga.

O projeto envolveu a definição dos requisitos técnicos, a integração e configuração do sensor LiDAR, o desenvolvimento de um algoritmo de estimação e a implementação da aquisição e processamento de dados em tempo real no PLC. Foram realizados testes para validar o desempenho da solução em condições experimentais. Os resultados demonstraram uma precisão promissora na estimativa de desvios horizontais e rotacionais, evidenciando, contudo, limitações na deteção de desvios verticais e falhas estruturais, devido às tolerâncias mecânicas e à resolução do sensor.

De forma global, a solução proposta contribui para aumentar a fiabilidade e a segurança das operações com SRMs, especialmente em armazéns automáticos de elevada densidade, estabelecendo uma base sólida para futuras melhorias, envolvendo sensores de maior resolução e algoritmos adaptativos.

Palavras-chave: LiDAR, PLC, SRM, Armazéns Automáticos

Acknowledgements

First of all, I would like to express my gratitude to Körber Supply Chain PT for their hospitality and for providing the opportunity to carry out this work. My immense gratitude goes to my company supervisor, João Gonçalves Costa, and to the entire team of the automation engineering department, who welcomed me from the very beginning of the project and offered support whenever needed.

I also wish to extend my sincere thanks to Professor António José Pessoa de Magalhães, whose contribution had a very positive impact on the final outcome of this dissertation, for all his support, commitment, availability, and patience in guiding me throughout this demanding project.

My appreciation goes as well to F.Fonseca for supplying the LiDAR sensor (multiScan165), an essential and key component for the success of this project, and for their readiness to provide technical assistance whenever required.

I am especially grateful to my family for providing me with the best conditions throughout my entire academic journey.

I would also like to thank all my friends who, in one way or another, offered support and motivation to complete this work.

Finally, I extend my deepest gratitude to my girlfriend, Mariana Andrade, for always being there during the most challenging moments and for continuously giving me encouragement and support to bring this dissertation to completion.

Thank you all very much.

Contents

List of Acronyms

AGV - Automated Guided Vehicle

AMR - Autonomous Mobile Robot

DB - Data Block

EPAL - European Pallet Association

FB - Function Block

FBD - Function Block Diagram

KSC PT – Körber Supply Chain PT

LAD - Ladder Logic

LiDAR - Light Detection and Ranging

PLC - Programmable Logic Controller

RADAR - Radio Detection and Ranging

RGV - Rail Guided Vehicle

RSSI - Received Signal Strength Indicator

SCL - Structured Control Language

SRM - Storage and Retrieval Machine

STL - Statement List

TCP - Transmission Control Protocol

TIA - Totally Integrated Automation

ToF - Time of Flight

UDP - User Datagram Protocol

VFD - Variable Frequency Drive

WCS - Warehouse Control System

List of Figures

List of Tables

1 Introduction

This chapter introduces the dissertation, starting with an overview of the host company, Körber Supply Chain PT, and its role in advancing automated systems in logistics and supply chain operations. It presents the background and motivation for the project, focusing on the challenges in automated warehouse operations. The objectives of the project are then outlined, aiming to develop a technological solution for pallet condition evaluation in SRMs (Storage and Retrieval Machines). Lastly, the dissertation structure is explained, presenting the upcoming chapters.

1.1 Presentation of the host company

Körber is a global technology group with around 13,000 employees across more than 100 locations. The company focuses on transforming entrepreneurial thinking into customer success by shaping technological change. In its business areas of Digital, Pharma, Supply Chain, and Technologies, Körber offers integrated products, solutions, and services that drive innovation and meet customer needs [1].

Körber Supply Chain PT (KSC PT) provides end-to-end software and automation solutions, specializing in the seamless integration of systems and processes throughout the supply chain. The company offers a wide range of solutions for automated warehouses, including SRMs, conveyors, Rail Guided Vehicles (RGVs), and Autonomous Guided Vehicles (AGVs). These solutions optimize warehouse operations, enhance efficiency, and improve material handling. With its expertise, KSC PT helps address today’s and tomorrow’s challenges, supporting supply chains worldwide.

1.2 Project background and motivation

The SRM, developed by KSC PT, plays a crucial role in automated warehouses, with the primary objective of efficiently moving and storing goods. These machines consist of an elevation unit that travels along a track, providing access to high-density shelving, thereby optimizing the use of vertical space. The main advantage of SRMs lies in the automation of storage and retrieval processes, which significantly enhances operational efficiency and minimizes human error. By automating these tasks, SRMs ensure the fast and precise handling of heavy loads, achieving a high storage rate and making the process faster and less reliant on manual intervention. The loads are transported on pallets, with the SRM loading and unloading them using its telescopic forks.

Despite their high complexity and capability of almost always interacting properly with loads and completing tasks successfully, collisions between the SRM's fork and the pallet occasionally occur. These collisions typically arise from misalignment between the pallet and the SRM or from structural faults in the pallet. When the goods being transported by the SRM are valuable and require extreme care—such as chemicals or pharmaceuticals—the consequences of pallet drops can result in substantial financial losses for the clients involved.

This project addresses that particular vulnerability present in KSC PT's SRMs. While the occurrence of accidents is rare, they do happen, and when they do, the company faces pressure from clients due to the significant financial damage that can arise from these incidents. This research aims to propose a potential technological solution that can mitigate this vulnerability by improving the SRM's ability to evaluate the pallets it handles. By enhancing the SRM's evaluation capabilities, the proposed solution will help KSC PT provide their clients with a more reliable system, ensuring greater confidence that accidents involving pallet drops will be prevented in the future.

1.3 Objectives of the dissertation

The main objective of this project is to study and develop a technological solution for SRMs that can detect and correct positioning deviations between the machine and the pallet, as well as identify structural faults in the pallet. The system will utilize LiDAR (Light Detection and Ranging) technology to capture accurate 3D data, enabling real-time estimation of positional misalignments such as horizontal, vertical, and rotational offsets, as well as the identification of structural pallet issues, such as broken or displaced parts, that could cause collisions with the SRM.

By integrating this solution into the SRM, it will enhance operational efficiency by reducing the need for manual interventions and minimizing the risks of pallet drops, especially for valuable or sensitive goods. The overall goal is to improve the safety, reliability, and precision of SRM operations in automated warehouses.

1.4 Organization of the document

This dissertation begins with the current chapter, which introduces the study. The second chapter addresses the project context, focusing on the challenges encountered in automated warehouses and SRMs, followed by a description of the proposed solution.

Chapter three starts with an introduction to the chosen technology, outlining its technical specifications. It then elaborates on the development of the algorithm designed to estimate the required pallet features.

In chapter four, the focus shifts to the system's implementation within the Siemens PLC (Programmable Logic Controller) environment. This chapter discusses the integration of the LiDAR sensor with the PLC, the program structure, execution flow, and the communication protocols employed.

Chapter five presents the experimental setup, testing methodology, and test cases along with their associated results, aimed at validating the performance of the proposed solution. The chapter concludes with a global discussion of the results, evaluating the system's effectiveness and identifying areas for improvement.

Finally, in the last chapter, the conclusions are presented, summarizing the key findings of the research and providing an overview of the strengths and weaknesses of the developed solution. It also explores potential directions for future work.

2 Problem definition and achievement expectations

This chapter aims to define the problem addressed in this dissertation and contextualize its relevance, providing the fundamental concepts necessary for its understanding, as well as an overview of the proposed approach to address it.

2.1 Project context

The present section provides an overview of the industrial environment in which the project is integrated. It outlines the main components and technologies involved in automated warehousing systems, with particular focus on SRM and their role within this context.

2.1.1 Automated warehouses

Automated warehouses have become a fundamental part of modern logistics, utilizing advanced machinery and software to optimize storage, retrieval, and distribution processes. Unlike traditional warehouses that rely heavily on manual labor, automated facilities integrate technologies such as conveyor systems, Automated Storage and Retrieval Systems (AS/RS), and Warehouse Management Systems (WMS) to enhance operational efficiency and accuracy. These systems enable high-density storage, improve inventory control, and minimize handling errors, contributing to a more streamlined supply chain [2].

The benefits of automated warehousing extend beyond efficiency improvements, providing significant cost savings, space optimization, and enhanced workplace safety. Automation leads to increased throughput, improved order accuracy, reduced labor costs, and enhanced operational efficiency, making it a strategic solution for companies looking to enhance their logistics capabilities. Automated systems allow warehouses to maximize space utilization through high-density storage solutions while reducing errors associated with manual handling. Additionally, automated material handling equipment decreases the physical strain on workers, reducing workplace injuries and enhancing overall safety standards. Despite the initial investment required for implementation, the long-term benefits of automation—such as lower labor costs, reduced processing times, and improved inventory accuracy—make it a valuable asset in modern supply chain management [2].

In the automated warehouses where KSC PT operates, several fundamental systems are implemented to ensure the proper functioning of the entire facility. The main components include SRMs, RGVs, autonomous vehicles that move along fixed rails to transport goods and conveyors, which are automated systems used to transfer handling units between different areas of the warehouse. Two common types of conveyors are roller conveyors, which use rotating rollers to move loads, and chain conveyors, which use chains to pull or push the load.

These warehouses are primarily designed for the storage of heavy loads and rely predominantly on pallets for material handling. The combined unit of the load and its supporting pallet is referred to as Handling Unit (HU).

A warehouse may accommodate multiple pallet types. Among the most commonly used are the "Euro pallet" (EPAL 1), the "closed industrial pallet" (EPAL 2), and the "open industrial pallet" (EPAL 3), shown in Figure 2.1.

Figure 2.1 - Commonly used pallet types [3]

HUs typically enter the warehouse via forklifts operated by warehouse operators, who place them onto the inbound conveyor. From that point onward, the process becomes fully automated, with HUs being transported by a series of conveyors that guide them through the system. Along this path, they may pass through various components such as elevators, particularly in multi-level warehouses, pallet inspection stations (described later), and other intermediate equipment.

When longer distances need to be covered within the warehouse, HUs can be transported by RGVs, for instance when transferring to a different operational area. Upon reaching the storage zone, they enter the SRM area, typically composed of high-density, parallel racking systems that can reach up to 40 meters in height. Between these racks, SRMs are positioned, usually one per aisle.

The pallets arrive at this zone via conveyors and stop at a predefined pick-up point where the SRM collects them. The load is then stored in the designated location within the racking system, as determined by the Warehouse Control System (WCS), which manages storage distribution and optimization.

2.1.2 Storage and Retrieval Machine engineering

SRMs are automated equipment designed for the efficient storage and transport of materials within warehouses and distribution centers. At KSC PT these machines are primarily used for handling pallets, ensuring a continuous and automated flow between the system's entry and exit points. An illustration of the machine is presented in Figure 2.2.

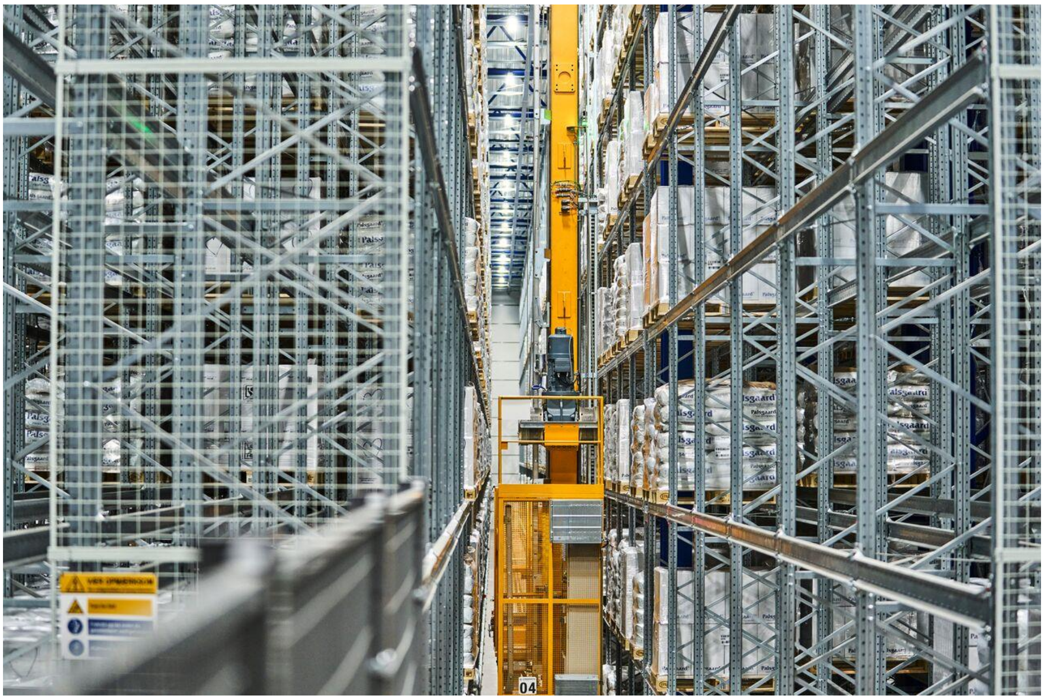

Figure 2.2 – SRM within an aisle of an automated warehouse

The operation of the SRM is based on integration with interface systems such as conveyors, allowing it to autonomously perform loading and unloading operations. The machine picks up a pallet from an inbound conveyor, positions it in a specific storage location, and later retrieves it for return to the conveyor system, enabling its exit from the system and delivery to the final destination.

SRMs not only maximize material transportation but also enhance warehouse organization and minimize the need for human interaction, resulting in more efficient operations.

Figure 2.3 illustrates the main components that make up a SRM. Other elements essential to its operation are also described in the following paragraphs.

Figure 2.3 - Main Structural Components of the SRM [4]

The SRM has 3 main axes, translation (x), hoisting (y) and fork (z). The main structural components of a SRM include the base, responsible for translational movement along a rail; the mast (or column), which enables the vertical hoisting of the platform; the platform, which transports the load and may contain telescopic fork or a satellite system; the rail, positioned on the floor to guide the crane's horizontal movement; and the upper guide, located at the top of the structure, providing stability during operation [5].

Each SRM receives loading, unloading, and positioning commands directly from the WCS and is controlled by a PLC. This controller manages communication with the WCS, monitors and controls the Variable Frequency Drivers (VFDs) for the translation, hoisting, and telescopic fork axes, processes signals from sensors and switches, and ensures operational safety, including monitoring the emergency chain [5].

The SRM's movement is driven by motors controlled by VFDs, which are installed in the onboard panel for the translation and hoisting axes, while the fork's movement is managed by an integrated motor-reducer VFD. Digital encoders, mounted on the translation and hoisting motors, provide feedback to the VFDs, ensuring a closed-loop control cycle. Any detected failure in the actuation system is reported to the PLC, which communicates with the VFDs via Profinet network, sending movement commands and collecting operational status [5].

Among the SRM sensors, the most relevant include load sensors, which continuously measure the weight on the platform and prevent movement if the limit is exceeded, and profile check sensors, which verify whether the HU dimensions comply with predefined limits. Additionally, inductive sensors detect the centered position of the fork, preventing unintended movements when activated [5].

For motion control, the system integrates magnetic limit switches for speed reduction in both translation and hoisting, as well as limit switches for these axes. These components ensure the safe and efficient operation of the SRM by preventing excessive acceleration, ensuring correct positioning, and detecting anomalies that could affect system performance [5].

The SRM positioning system utilizes laser measurement encoders for translation (X) and hoisting (Y), ensuring high precision and safety in movement. In both axes, a fixed optical sensor measures the distance to a moving reflector, achieving a ±1 mm resolution without requiring reference points. These encoders are connected to the VFDs, enabling position control, with continuous data transmission to the PLC via Profinet [5].

For fork positioning (Z-axis), the system uses an absolute rotary encoder directly coupled to the motor shaft, ensuring precise control over the linear displacement of the telescopic fork [5].

2.2 Problem overview

Despite the high technological advancements in the KSC PT's products, particularly in SRMs, accidents involving pallets falling with goods still occur more frequently than the desired. These incidents typically result from collisions between the SRM and the pallet, which can be attributed to various factors such as SRM positioning deviations, pallet positioning deviations (rotation, lateral or vertical offset), and damaged pallets.

According to an email received (P. Andrade, personal communication, Mar. 13, 2025), in 2024, Super Bock Group reported a financial loss associated with pallet falls. Beyond the financial impact of damaged goods, these incidents pose a significant operational risk, potentially leading to accidents involving operators and structural damage to both the warehouse and machinery. Figure 2.4 shows the consequences of an accident.

To make things worse, some KSC PT clients store chemical and pharmaceutical products, where the risks and losses associated with pallet falls are even more critical. In these cases, ensuring high precision in the relative positioning between the load and the SRMs is essential to prevent incidents that could compromise safety and operational integrity.

Figure 2.4 - Falling pallet with goods

SRMs are influenced by various internal and external factors that may cause misalignment between the machine and the HU, leading to positioning errors. One of the main causes is wear on the SRM guide rollers, which results in machine inclination.

Pallet positioning deviations can occur due to rotation (example shown in Figure 2.5), lateral offset or vertical offset. Rotation may be caused by looseness in the fork mechanisms, particularly due to backlash in the gearbox, or defects such as protrusions on the pallet, which may collide with the SRM during unloading, leaving it misaligned. Lateral offset of the pallet can result from displacement of the stopper on the last conveyor before the pallet is loaded onto the SRM, or variations in SRM positioning when picking up the pallet from the conveyor. These last two factors often lead to horizontal misalignment of the fork within the pallet tunnels, causing improper placement in the rack. Vertical offset of the pallet, that is, a variation in the relative height between the pallet and the SRM, can result from deformations in the warehouse racking structure.

Figure 2.5 - Rotated pallet

In addition to positioning deviations, pallet quality is also crucial for the proper functioning of the system. To ensure compliance, several pallet verification stations are distributed throughout the warehouse, where HUs undergo inspection. An example of one of these stations is shown in Figure 2.6, it checks various parameters such as dimensions, weight, hole geometry, and the condition of the pallet boards.

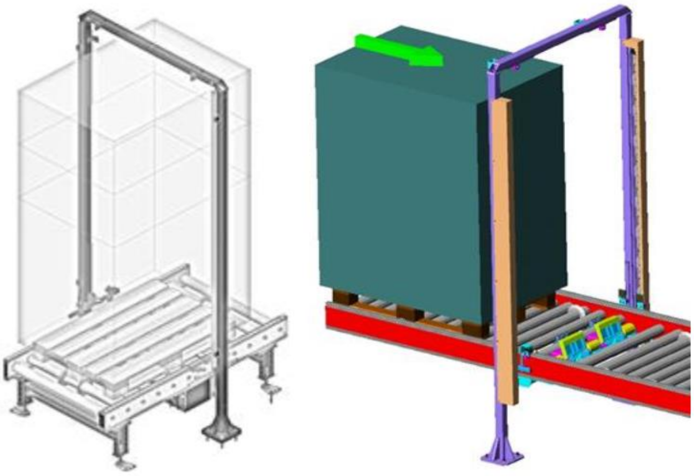

Figure 2.6 - Pallet inspection station [6]

Despite these control measures, damaged pallets, such as those with broken boards, may still reach the SRM and storage racks. One example of this type of pallets is presented in Figure 2.7. These defects can develop due to collisions during transport within the warehouse. When a pallet encounters an issue, such as getting stuck, an operator is alerted to intervene and reintroduce it into the system. However, during these interventions, sometimes involving the use of force, the pallet may become damaged without the operator realizing it.

For this reason, any additional verification measures that help anticipate pallet-related issues are a valuable enhancement to the system's reliability.

Figure 2.7 - Damaged pallet

2.3 Current fine positioning system

Currently, there is no solution in place within the KSC PT’s SRMs that allows for analyzing the position and geometry of the pallet before loading. The system simply provides the SRM with the coordinates of the rack where the target pallet is located, and the machine moves there to load it, assuming that the pallet is correctly positioned. However, if the pallet happens to be misaligned, the fork will likely collide with it when advancing.

There is, however, a fine-positioning control solution for SRMs, occasionally used in applications requiring high precision. Although this system does not read the exact position of the pallet, it enables the SRM to align itself with high accuracy relative to a reference marker on the rack beam where the pallets are stored. This solution consists of a camera mounted on the SRM platform, facing the rack. While the camera has limited image processing capabilities, its sole function is to detect a target embedded in the rack beam and use it as a reference to center the SRM in the correct position for loading and unloading pallets.

This approach is particularly robust in cases of rack deformations, a common issue due to the significant variations in stored loads, which can cause structural shifts. Since pallets move along with the beams in such cases, ensuring correct positioning relative to the beam also ensures alignment with the pallet itself. For example, if the rack is deformed, the camera detects that the target is misaligned and commands the SRM to adjust its position accordingly until it is correctly aligned with the target.

This fine-positioning system is also capable of correcting misalignment errors when they originate from the SRM itself.

In summary, this solution ensures correct relative positioning between the SRM and the pallet, as long as the pallet is properly aligned with the reference target on the rack beam. However, this system does not detect pallet defects, rotational, horizontal or vertical offsets relative to the reference position on the rack beam.

2.4 Proposal for solving the problem

This section presents a LiDAR-based solution to the problem of identifying position discrepancies between SRMs and the pallets they handle. It outlines the rationale behind the selection of LiDAR, emphasizing its precision in object detection and distance measurement. The intended implementation steps are also described in this part, along with the main achievements expected.

2.4.1 Project expectations for LiDAR deployment

LiDAR is an advanced sensing technology that employs laser pulses to measure distances with high precision, enabling the creation of detailed 2D and 3D spatial maps of the environment. It functions by emitting laser pulses and measuring the Time-of-Flight (ToF), the time taken for the reflected pulse to return to the sensor, allowing for accurate distance calculations and environmental reconstruction. This ToF technology has emerged as a focal point of research within the realm of 3D imaging. Owing to its relatively straightforward principles and exceptional performance, ToF technology finds extensive applications across various domains including human-computer interaction, autonomous driving, industrial inspection, medical and healthcare, augmented reality, smart homes, and 3D reconstruction, among others [7].

LiDAR sensors have been widely used in industrial applications for decades, playing a crucial role in automation and safety. These sensors operate both indoors and outdoors, facilitating port automation, traffic management, and object protection. Their versatility makes them essential for Industry 4.0 applications [7].

Inspired by RADAR (Radio Detection and Ranging) technology, LiDAR enables non-contact distance measurement using laser-based sensors. These sensors are available in 1D, 2D, and 3D variants, each serving different industrial needs. 1D LiDAR sensors measure distance to a specific target or reflector. 2D LiDAR sensors capture distance and angular data by rotating on a single plane, generating sequential measurements over time. 3D LiDAR sensors add a third dimension by pivoting or using multi-layer scanning, providing spatial data along the X, Y, and

Z axes, enabling applications in autonomous navigation, object detection, and robotic mapping [8].

In the past ten years, 3D LiDAR has received more and more attention, which can be seen from the number of relevant papers published, the amount of capital investment and the number of industry players involved. Compared with classic 2D LiDARs, modern 3D LiDARs not only add a extra spatial dimension by increasing the number of scanning layers, but also achieve wider fields of view and range. Nowadays it´s possible to find 3D LiDARs with 360-degree scanning and a measurement range of up to 300 meters [9].

LiDAR technology is increasingly being adopted in logistics systems, serving a crucial role in autonomous navigation and operational safety. It enables the advancement of autonomous vehicles and equipment, ensuring more reliable and efficient operation.

A significant study on the application of LiDAR in KSC PT’s logistics systems was conducted by Regado exploring the implementation of this technology to enhance navigation and safety in RGVs. The research demonstrated that LiDAR not only provides reliable obstacle detection but also enables precise distance measurement and environmental variation analysis—essential factors for optimizing the movement of industrial vehicles [10].

The Regado’s study involved the implementation of the SICK TIM781-2174101 LiDAR sensor, where experimental validation confirmed its measurement accuracy, ensuring average errors below 20 mm. Beyond precise detection, the findings highlighted how LiDAR enhances industrial vehicle navigation by supplying real-time data for trajectory adjustments. Its ability to quickly identify obstacles allows RGVs to operate with greater predictability and safety, minimizing collision risks and improving logistical flow [10].

During the research phase on the potential use of LiDAR, efforts were made to identify applications closely related to the present case, particularly involving LiDAR integration in SRMs. However, no relevant studies were found with premises and objectives similar to the present study. Nevertheless, the research conducted by Regado proved to be closely related to the current work.

Based on Regado’s research, it is evident that LiDAR is highly beneficial for logistics applications, ensuring measurement accuracy, efficient obstacle detection, and significant improvements in navigation and equipment safety. Its ability to function in dynamic industrial environments makes it a strategic choice for systems requiring precise position control and load movement, such as SRMs. Therefore, the application of LiDAR in this study aligns with previously established literature, reinforcing its importance in the evolution of automated logistics systems [10].

2.4.2 Project development stages and goals

The development of the project is structured in three main phases: Problem Analysis and Conceptual Definition, Development, and Testing and Validation. Each phase consists of distinct stages aimed at progressively building a robust solution for the pallet verification task using a LiDAR sensor integrated into the SRM system.

The first phase begins with the definition of the technical requirements for the sensing system, including the necessary measurement range, precision, resolution, field of view and environmental constraints. Based on these specifications, a market analysis is conducted to identify available LiDAR technologies capable of meeting these requirements. Following the sensor selection, the conceptual design of the system is established, defining the positioning of the sensor, expected data outputs, and general interaction with the SRM’s control architecture.

The second phase, Development, is conducted entirely in a controlled office environment and is structured into four main stages. It begins with the integration and initial configuration of the LiDAR sensor, during which the device is set up using appropriate software and the first telegrams are received and analyzed. This initial step aims to verify the correct functioning of the sensor and to understand the structure of the measurement data. Following this, the sensor is connected to a Siemens PLC, and communication protocols are implemented to allow the transmission of commands and the reception of real-time data, establishing the foundation for later automation. Once communication is established, a data acquisition and pre-processing system is developed within the PLC to handle the incoming data, apply initial filtering, and organize it for further analysis. Finally, the pallet evaluation program is developed and implemented within the PLC to estimate different pallet features, such as horizontal or vertical offsets, rotation, or structural faults, based on the processed LiDAR data.

The third and final phase, Testing and Validation, consists of running the complete program on the PLC in an experimental environment to verify whether the LiDAR system effectively estimates the intended pallet characteristics. These tests aim to validate the accuracy and reliability of the developed solution under controlled conditions, ensuring that the system correctly identifies situations such as misalignments or structural anomalies.

2.4.3 Main achievements expected

The project aims to demonstrate the feasibility of integrating a 3D LiDAR sensor into a warehouse automation system to enhance the pallet verification process in SRMs. The main expected achievements include the successful configuration and communication of the LiDAR sensor with a Siemens PLC using standardized protocols, as well as the development of a reliable algorithm capable of detecting key pallet characteristics, such as horizontal and vertical misalignment, rotation, or structural faults. One of the most demanding aspects of the project lies in the ability to process, within the PLC, the large volume of data generated by the LiDAR point cloud. This requires a strategic selection of relevant data and careful optimization of the algorithm to ensure efficient handling and real-time performance. Additionally, the system is expected to be validated through experimental testing, confirming its ability to provide accurate and consistent detection results under controlled conditions. These outcomes are intended to contribute to improved automation and greater operational reliability, paving the way for potential real-time pallet verification in future warehouse applications.

2.5 Summary

This chapter outlined the context and motivation of the project, highlighting the relevance of SRMs in automated warehouse systems and the limitations of the current fine positioning approach, particularly the inability to detect pallet misalignments or structural faults. Such limitations may result in incidents like collisions or load drops, with serious implications for safety and operational efficiency. To address this, a LiDAR-based solution was proposed to enable real-time verification of pallet conditions and enhance system reliability.

The development process is organized into distinct phases, from requirement specification to experimental validation. The core objectives include establishing communication between the LiDAR and a PLC, designing a data acquisition and processing algorithm, and validating the system’s effectiveness in improving pallet verification.

The next chapter will focus on the development of the proposed solution, covering the configuration of the selected sensor and a description of its functionality. It will then explain the strategies that comprise the algorithm capable of evaluating the pallet's structural and positional condition.

3 MultiScan165 description and algorithm development for pallet feature estimation

This chapter focuses on the development of the pallet evaluation proposed solution, beginning with the description of the LiDAR sensor. It covers its measurement principles, coordinate system, filtering capabilities, and data output format, which are essential for understanding how the measurements are processed. The chapter then explains the algorithms developed to estimate the pallet's position and structural integrity, detailing how the operational data model was structured to support the estimation functions.

3.1 Technology selection: the SICK multiScan165

Several factors were considered when selecting the LiDAR to be used. First and foremost, the technical requirements of the application were taken into account. However, there was also the constraint of needing a supplier willing to provide access to the equipment for an extended period, since the main goal of this project was to develop a functional program and implement it in practice, effectively testing the reliability and performance of the chosen sensor. Table 3.1 presents the main LiDAR requirements defined for this application.

Table 3.1 – LiDAR requirements

Parameter	Requirement
Sensor type	3D LiDAR (multi-layer)
Application environment	Industrial (dust, vibration, variable lighting)
Measurement range	100–2000 mm
Statistical error	≤ 10 mm
Horizontal aperture angle	≥ 160°
Vertical aperture angle	≥ 35º
Communication protocol	Ethernet-based
Integration capability	Real-time data acquisition via PLC

The sensor selected for this application had to be a 3D LiDAR, in order to enable spatial analysis of the scene. A 2D LiDAR would allow only a single horizontal plane to be analyzed, which could be sufficient to assess the pallet's horizontal alignment. However, it would not provide information about vertical alignment unless a scan in motion was performed to capture multiple planes and reconstruct a 3D view of the scenario. This approach, however, would increase data acquisition time and consequently extend the SRM's loading cycle time. Moreover, a 2D solution would not allow the detection of structural faults in the pallet that could compromise the loading process.

Another constraint in this application that significantly limits the range of possible vision systems is the short distance between the SRM and the rack where the pallet is located. This distance varies between 100 mm and 200 mm. Considering that the pallet can be up to 1000 mm wide, and that some lateral displacement must be tolerated, the system requires a horizontal aperture angle of at least 160° to capture the full width of the pallet. Regarding the vertical aperture angle, in order to capture the relevant portion of the pallet height, namely the tunnels along with some tolerance for displacement, a minimum of 35° is required.

The selected LiDAR sensor was the multiScan165 from SICK [11]. This is a compact and robust 3D LiDAR device specifically suited for demanding industrial environments, making it highly suitable for applications such as pallet condition monitoring in automated warehouses. It features 16 scan layers with a 360° horizontal field of view and a vertical aperture angle of 42°, covering from -7.5° to +35°. The sensor provides a horizontal angular resolution of 0.5° and a vertical resolution of approximately 2.5°. The working range reaches up to 62 meters, although for near-field measurements, such as those required in this application, it maintains high accuracy. The statistical error is ≤10 mm, supporting precise detection even at short distances [11].

Engineered for industrial resilience, the SICK multiScan165 exhibits excellent environmental robustness. It is designed to operate under wide temperature ranges (–40 °C to +50 °C) and tolerate strong mechanical stress, including vibration (up to 5 g) and shock (up to 50 g), as certified by IEC 60068 standards. Additionally, its IP69/IP65 ratings ensure full protection against dust and high-pressure water, confirming its suitability for harsh industrial environments [11].

Communication is handled via Ethernet with support for TCP/IP and UDP/IP, ensuring integration into automation systems such as PLCs. In addition to raw measurement data output, the sensor supports an integrated 3D Object Detection function based on Field Evaluation, which enables onboard detection logic. Furthermore, it includes optional digital add-ons such as multi-echo processing and basic filtering features to enhance signal reliability in complex scenes [11].

The sensor can be fully configured via SICK SOPAS Air, a browser-based software tool that enables easy adjustment of sensor parameters according to application requirements.

3.2 MultiScan operating principles and data format

An overview of the multiScan sensor's basic working principles and the format of its output data is given in this part. Both are crucial for understanding how the sensor is integrated and used in the developed system. The measuring principle that the sensor uses is explained first, then the coordinate system that is used to understand the spatial data. Important features are also introduced, including the Field Evaluation feature, which is utilized for real-time object detection, and built-in filtering algorithms. Lastly, the measurement data's structure and transmission format are described in detail, providing the basis for its processing and decoding within the PLC environment.

3.2.1 Measurement principle

The device is an opto-electronic LiDAR sensor that performs non-contact scanning of its environment using laser beams. Measurements are acquired in spherical coordinates, referenced to the sensor's measurement origin, which is physically indicated by a circular indentation at the center of the optics cover. When a laser beam intersects an object, the sensor determines its position by calculating the corresponding distance and angular coordinates. Figure 3.1 shows the multiScan scanning an object [12].

Figure 3.1 - Device with 16 scan layers, side view [12]

The device has a total of 16 scan layers. One of them is a planar scan layer positioned at a 0° elevation angle, which is specifically intended to assist accurate navigation tasks.
The remaining 15 layers are conical, with 2 oriented downwards and 13 upwards. Figures 3.2 and 3.3 illustrate the vertical distribution and spatial orientation of the multiScan's scan layers [12].

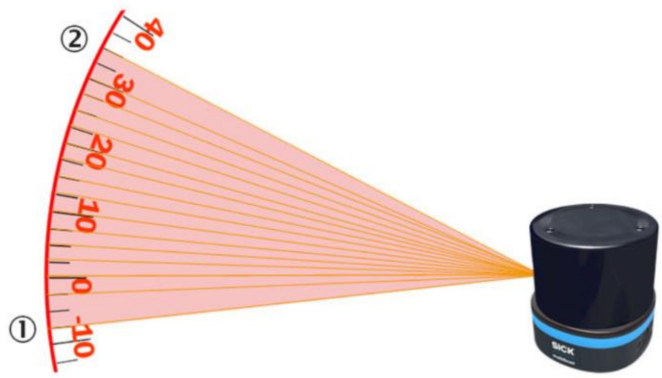

Figure 3.2 - Side view illustrating the angular distribution of the 16 scan layers of the sensor, ranging from scan layer 1 at –7.5° to scan layer 16 at +35° [12]

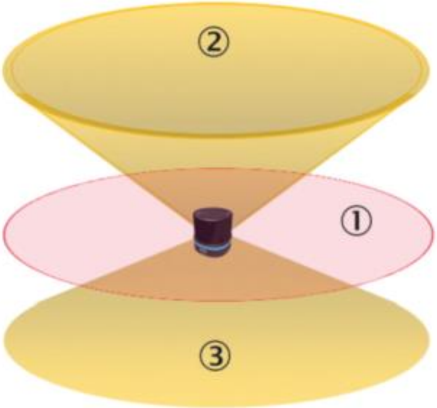

Figure 3.3 - Three-dimensional representation of the possible orientations of scan layers: (1) a horizontal scan layer with 0° elevation; (2) upward-facing layers with negative elevation angles; and (3) downward-facing layers with positive elevation angles [12]

The device measures distance by emitting pulsed laser beams via a laser diode. When a beam is reflected by an object, the sensor detects the returning signal. The distance to the object is then calculated based on the time of flight, that is, the time elapsed between the emission of the pulse and the reception of its reflection, as suggested by Figure 3.4 [12].

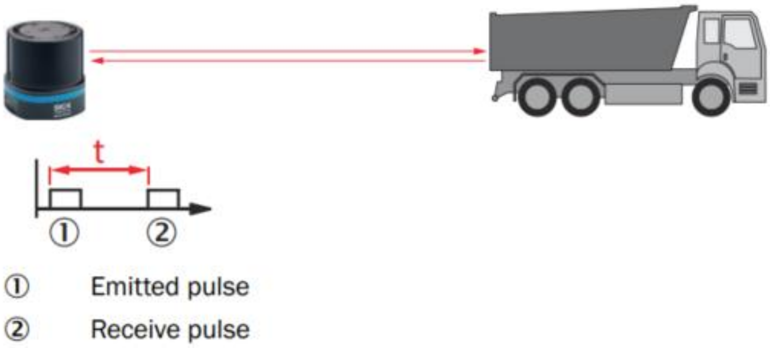

Figure 3.4 - Time-of-Flight Principle for Distance Measurement [12]

3.2.2 Coordinate system

The device coordinate system is defined with its origin at the point (x=0, y=0, z=0), which serves as the reference for all emitted laser beams and corresponding distance measurements. In the absence of any translation relative to the world coordinate system, this origin coincides with the world coordinate origin. The horizontal angular position of each beam is referred to as θ (azimuthal angle). The beam with a θ value of zero lies at the center of the device's main viewing direction, as shown in Figure 3.5 [12].

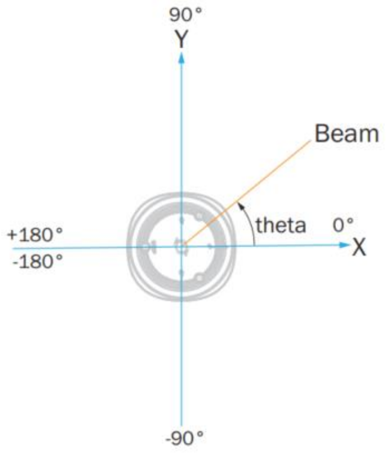

Figure 3.5 - Device coordinate system and definition of azimuthal angle θ in the *X-Y* plane, with 0° along positive *x* and angles increasing counterclockwise [12]

The elevation angle, also referred to as the vertical angle, is denoted by the symbol ϕ and is defined relative to the device's *x–y* plane. A value of ϕ less than zero ($\phi < 0$) indicates a direction above the *x–y* plane, corresponding to positive *z* values, whereas a value greater than zero ($\phi > 0$) indicates a direction below the *x–y* plane, toward negative *z* values. This is visually represented in Figure 3.6. It is important to note that all measurement data are expressed in the device's coordinate system, rather than in a global or world coordinate reference frame [12].

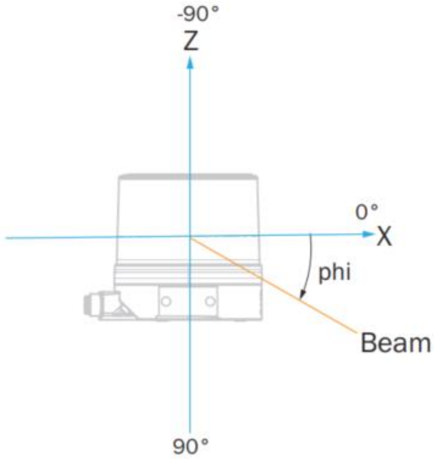

Figure 3.6 - Definition of the elevation angle ϕ in the device coordinate system [12]

The world coordinate system is based on the DIN ISO 8855 standard. The rotational directions follow a clockwise coordinate system. The yaw, pitch, and roll angles specify the device's orientation in the world coordinate system, while the Cartesian coordinates *x*, *y*, and *z* specify its position. If no difference between the world and device coordinate systems is defined, such as for defining a precise mounting position, the origins of both coordinate systems are the same and correspond to the device's origin [12].

The alignment of the device is defined with respect to its internal coordinate system. The laser beam with an azimuthal angle (θ) of 0° and an elevation angle (ϕ) of 0° is directed along the positive *x*-axis. The scan layer corresponding to an elevation angle of 0° lies exactly within the *x-y* plane. The origin of the device coordinate system is assumed to coincide with the origin of the world coordinate system. Furthermore, the top of the device is oriented toward increasing *z*-values. The direction of rotation is determined by the device's orientation, with θ representing the yaw angle and ϕ the pitch angle [12].

3.2.3 Filters

The SICK multiScan165 is equipped with a comprehensive set of configurable filters designed to enhance measurement reliability and optimize data processing. These filters play a crucial role in suppressing noise, excluding irrelevant information, and focusing computation on spatially meaningful data. All filter configurations are managed through SICK SOPAS Air, a browser-based software tool. As a result, the filters contribute to more accurate measurements and improved overall system performance, particularly in complex or dynamic environments [12].

The fog filter mitigates false detections by suppressing unwanted echoes at close range, which are common in foggy conditions. The echo filter removes reflections caused by environmental disturbances such as rain, dust, snow, or edge hits. It allows the user to configure which echoes are output—only the first, the last, or all available reflections [12].

As shown in Figure 3.7 (left part) without the use of an echo filter, the device registers multiple unwanted echoes resulting from ambient conditions, such as rain. These parasitic reflections can interfere with accurate distance measurements. When the echo filter is activated (configured to detect the last echo), the device is able to suppress unwanted reflections caused by environmental interference, as represented in right part of Figure 3.7.

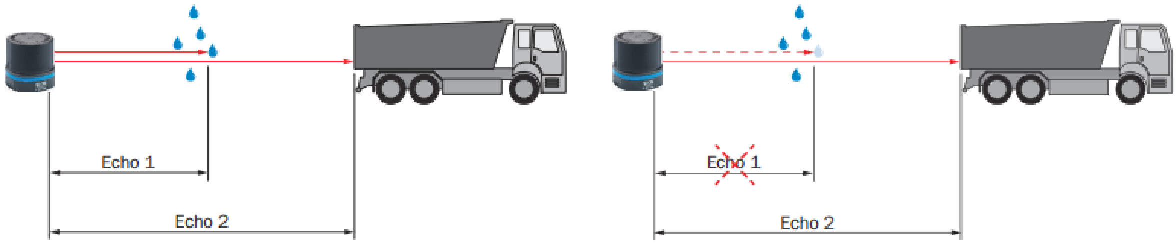

Figure 3.7 - Effect of echo filter on measurement accuracy [12]

The particle filter is designed to ignore small, transient reflections from particles like dust, raindrops, or snowflakes. It evaluates sequential scans and discards measurement points that deviate significantly from their spatial or temporal context. The moving average filter improves signal stability by averaging a configurable number of scans per point. While this reduces measurement noise, it introduces a corresponding delay proportional to the number of averaging cycles [12].

In addition to signal-level filters, the multiScan165 also provides data reduction filters aimed at optimizing processing efficiency. The scan layer filter allows selective deactivation of specific scan layers, while the scan range filter restricts the horizontal angular output to a user-defined interval between –180° and +180°, with 0° aligned to the front of the device. Data outside the specified range is excluded, and partially included data is zero-filled to maintain structure [12].

Finally, the distance filter defines a spherical measurement zone around the device by setting minimum and maximum radial distances. Instead of removing data outside this range, it assigns a value of zero, allowing for the isolation of a solid region, a hollow shell, or an exclusion zone depending on the configuration. This is particularly useful when measurements are only relevant within a specific spatial boundary [12].

3.2.4 Field evaluation

The device features an integrated field evaluation function that enables the monitoring of predefined zones within its scanning area. This functionality is particularly useful for applications such as collision avoidance, object protection, and access control. These zones are defined as volumetric fields, which can be created and configured by the user through the SOPAS software. Once configured, these fields can be linked to specific digital outputs of the device, which are triggered whenever an object enters or obstructs the defined volume [12].

Up to 48 independent fields can be defined, and the evaluation logic can be combined with other input signals using logical operators such as AND, OR, or XOR. This allows for flexible and application-specific control strategies [12].

As illustrated in Figure 3.8 two fields are configured; the field on the right is currently active due to the presence of an object within its boundaries.

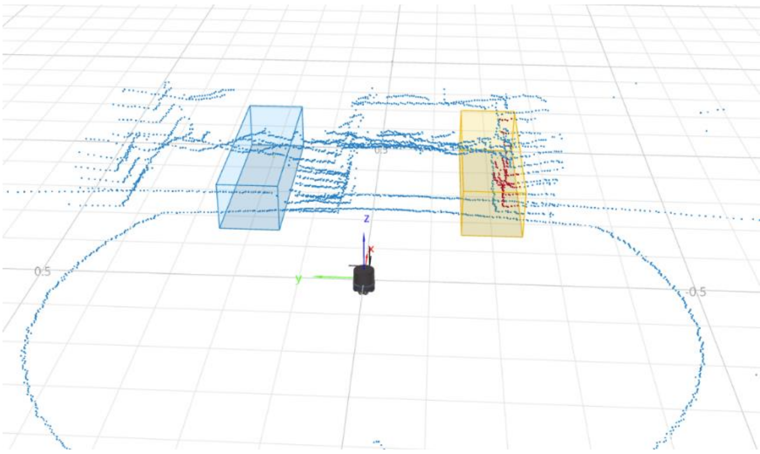

Figure 3.8 - Application of the Field Evaluation Function in SOPAS Air

The minimum detectable object size by the SICK multiScan165 depends on both the distance to the object and the angular resolution of the device. According to the official documentation, the smallest object at a desired distance that can still be reliably detected is shown in Table 3.2.

Table 3.2 - Typical minimum object size [mm] as a function of distance and angular resolution [12]

Angular resolution [α_{res}]	Horizontal 0.5°	Vertical 2.5°	Vertical 5,0° [1)]
Distance [mm]			
100	13	13	13
200	13	13	19
500	13	26	47
1000	16	51	95
2000	32	102	190

1) between scan layer 1 and 2 / scan layer 15 and 16

3.2.5 Measurement data output

The device supports two data output formats—MSGPACK and Compact—both transmitting data segment by segment via UDP and including essential metadata such as timestamps and segment serial numbers. MSGPACK offers greater readability and ease of parsing due to its structured format with descriptive field names, and benefits from existing library support. However, it requires higher computational resources and greater bandwidth. In contrast, the Compact format is more efficient in terms of data size and transmission, although it lacks descriptive structure and may require additional integration effort [13].

Given that data processing is performed on a PLC, which offers limited support for external libraries and reduced flexibility for handling complex data structures, the Compact format was selected. Its reduced size and simplicity make it more suitable for real-time processing in environments with constrained computational resources.

The multiScan is equipped with two independent measuring modules that operate in parallel to acquire data across its 16 scan layers. Each module is responsible for a specific subset of layers, as shown in Table 3.3, which also presents the corresponding elevation angles for each layer.

Table 3.3 - Scan layer allocation and corresponding elevation angles [12]

Scan layer	Measuring module allocation to scan layers	DIN ISO 8855	Physical
1	Measuring module 0	7.3°	-7.3°
2	Measuring module 0	2.4°	-2.4°
3	Measuring module 0	0.0°	-0.0°
4	Measuring module 0	-2.5°	2.5°
5	Measuring module 1	-5.4°	5.4°
6	Measuring module 0	-7.4°	7.4°
7	Measuring module 1	-10°	10°
8	Measuring module 0	-12.5°	12.5°
9	Measuring module 1	-14.7°	14.7°
10	Measuring module 0	-17.5°	17.5°
11	Measuring module 1	-19.6°	19.6°
12	Measuring module 0	-22.7°	22.7°
13	Measuring module 1	-24.7°	24.7°
14	Measuring module 1	-27.3°	27.3°
15	Measuring module 1	-29.9°	29.9°
16	Measuring module 1	-35.3°	35.3°

Each layer is associated with a specific elevation angle (ϕ), measured according to the DIN ISO 8855 convention. The angular separation between layers is approximately 2.5°, resulting in a total vertical field of view of 42.6°.

The device transmits measurement data using segment-based telegrams. The data is structured in frames, each composed by segments representing 30° portions of the 360° scan. These segments include distance values for each beam, as well as RSSI value, azimuth angle, among other data, encoded in the selected output format. Each segment contain the data of all scan layers for a smaller azimuth interval (30º). A full 360° scan requires the reception and processing of all 12 segments [12].

Figure 3.9 illustrates the angular distribution of the 12 segments associated with Measuring Module 0, each covering 30° of the 360° scan.

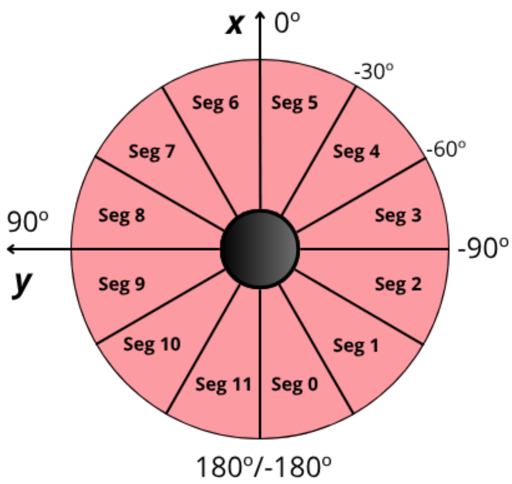

Figure 3.9 - Angular distribution of the segments corresponding to Measuring Module 0

The data packets transmitted in Compact format are enclosed in a frame consisting of a header before the actual payload and a checksum after the payload, as illustrated in Figure 3.10 [13].

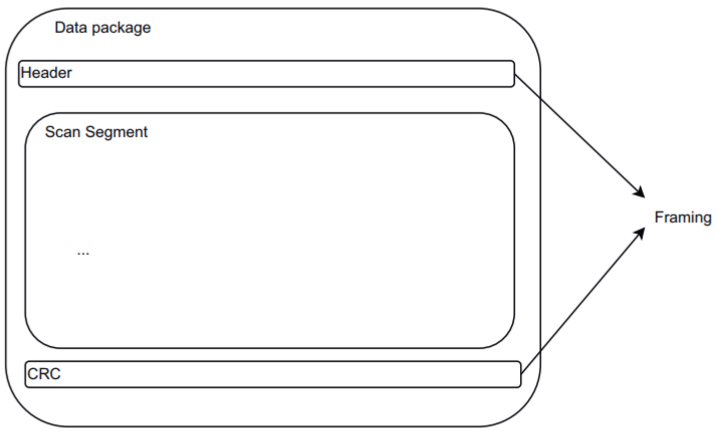

Figure 3.10 - Framing in the Compact format [13]

Each data packet, or telegram, consists of a fixed-structure byte sequence encoded in little-endian format, where each group of bytes corresponds to a specific parameter or piece of information. Some of the most relevant fields contained within these telegrams are presented as follows [13].

Each telegram begins with a fixed header containing essential control and synchronization fields. The “startOfFrame” field marks the beginning of the telegram using a specific byte pattern, allowing the receiver to correctly identify the start of the data structure. The “timeStampTransmit” field provides the precise system time at which the telegram was generated, enabling accurate temporal alignment of the measurements. Additionally, fields such as “sizeModule0” indicate the length of the subsequent data block associated with a specific measuring module. These elements structure the telegram and prepare the data stream for parsing of the metadata and measurement values that follow [13].

As illustrated in Figure 3.11, each module within a scan segment contains two main components: first, the metadata, which describes the structure and context of the data, and then the measurement data, which includes the actual distance values recorded by the sensor. This organization allows the processing system to interpret and associate each measurement correctly.

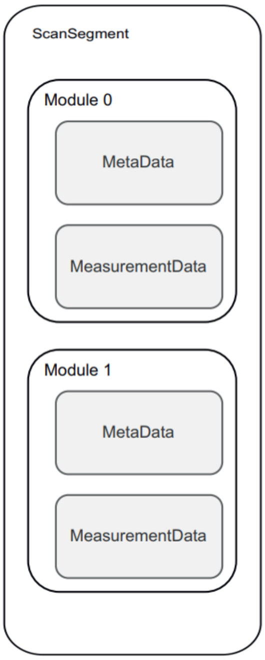

Figure 3.11 - Metadata and measurement data in the individual modules [13]

Each module's metadata includes several fields that describe the context of the corresponding measurement data. The "SegmentCounter" (uint64, 8 bytes) identifies the sequence of segments within a complete 360° scan, allowing each segment to be associated with a specific angular portion of the scan. The "numberOfLinesInModule" (uint32, 4 bytes) specifies how many scan layers are included in the current module [13].

The "Phi" field is an array of elevation angles (float32, 4 bytes per element), where the number of elements corresponds to the number of layers in that module. Similarly, the "ThetaStart" and "ThetaStop" fields are arrays of azimuth angles (float32, 4 bytes per element) representing the start and end angle of each scan line, respectively. These angular fields are essential for spatially locating each measurement within the 3D point cloud. Among other metadata elements, they provide the necessary information to correctly reconstruct and interpret the measurement data [13].

The measurement data section contains the actual values acquired by the sensor for each beam. The "Distance" field (uint16, 2 bytes) represents the measured distance in millimetres. The "RSSI" (Received Signal Strength Indicator) field (uint16, 2 bytes) indicates the strength of the received signal, providing an additional measure of measurement reliability. The "Azimuth angle (theta)" field (uint16, 2 bytes) encodes the horizontal angle of each measurement beam. These data fields are structured sequentially for each echo and scan layer, enabling the precise reconstruction of the 3D environment [13].

3.3 Pallet position checking algorithms

Finally, the core algorithms responsible for analyzing the multiScan data were defined. Based on the spatial distribution of the measured points, the system is able to detect and interpret features such as horizontal and vertical offsets, rotations and structural pallet faults.

This section begins by presenting the positional context of the main elements involved in the system, and concludes with a description of the estimation functions used to evaluate the relevant pallet features. It is important to note that all coordinate references used throughout this section are based on the multiScan coordinate system.

3.3.1 Typical baseline dimensions and sensor positioning

In this section, the typical dimensions relevant to the problem in real-world warehouses are presented. Although these values may vary slightly across different warehouses and applications, they represent typical average dimensions observed in multiple real-world cases. These dimensions include the relative positioning between the pallet, the multiScan sensor, and the SRM. While suitable for simulation and prototype validation, it should be noted that, in any potential future implementations, these parameters must be adapted to the specific characteristics of the deployment environment.

Figures 3.12, 3.13, and 3.14 show the top, front, and side views of the system, respectively, where the key elements of the problem can be identified: the pallet, the rack, the multiScan sensor, and the SRM, along with their relative positioning.

Notable aspects include the horizontal and vertical aperture angles, as well as the clearances between the fork and the pallet tunnels, 50 mm of lateral clearance on each side, and vertical clearances of 20 mm above the pallet and 10 mm below it, relative to the bottom beam.

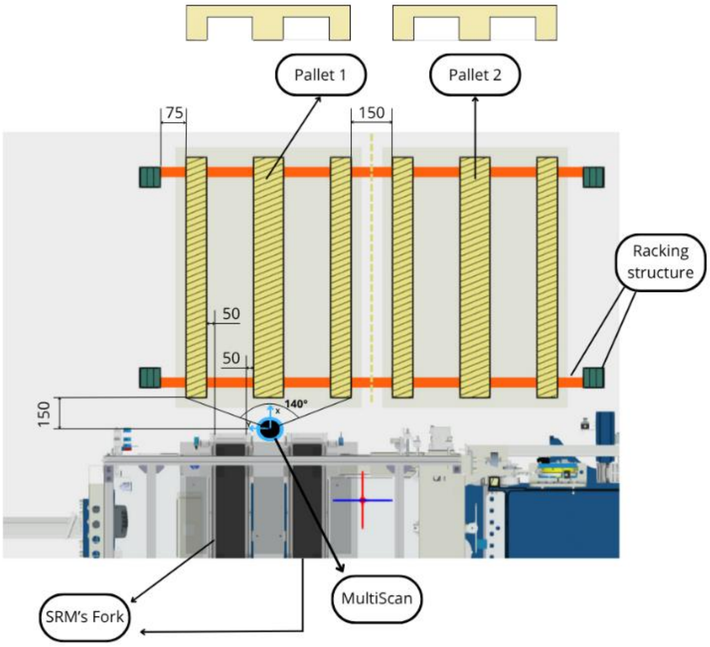

Figure 3.12 - Top view of the system, including the SRM, pallets, the multiScan, and the rack

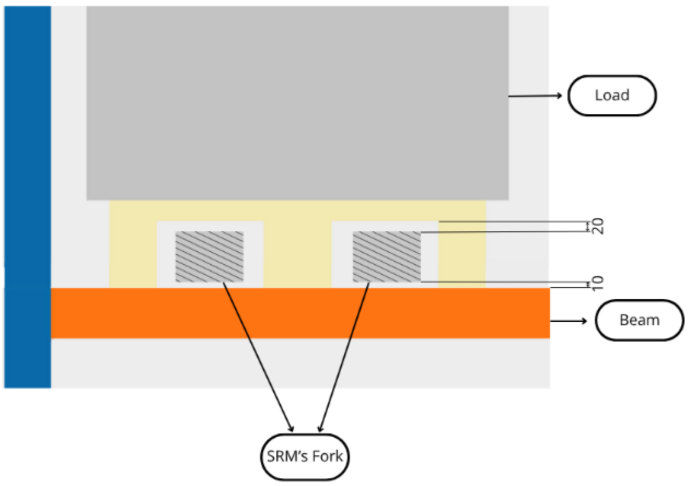

Figure 3.13 - Front view of the system, including the SRM's fork, pallet with load and the rack

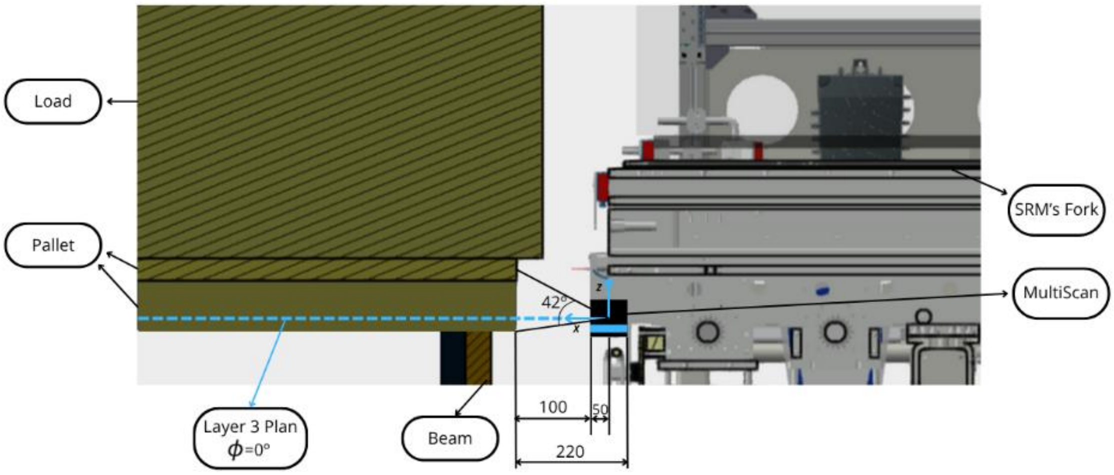

Figure 3.14 - Side view of the system, including the SRM, pallet with load, multiScan, and the rack

Figure 3.14 shows a cross-section of the SRM platform, highlighting the telescopic fork, which moves along the x-axis and inserts into the pallet tunnels to perform the loading operation when requested.

3.3.2 Definition of the Operational Data Model

This section describes the structured format of the measurement data after pre-processing by the PLC, which is subsequently used by the estimation algorithms implemented in the system. The primary goal is to convert raw multiScan data into a clean, compact input vector suitable for consistent and efficient feature estimation. Two distinct data models are defined: one for the horizontal evaluation phase and another for the vertical evaluation phase.

For the horizontal evaluation phase, the PLC receives raw measurement segments from the multiScan and filters the data to retain only the distance values corresponding to a horizontal angular range of 180°. These values are extracted from the horizontal scan layer (0° elevation), which provides a planar representation of the pallet's front profile.

The resulting horizontal data model is defined as a vector of 180 integer values, each of which representing the measured target distance in millimeters. The radial resolution was intentionally limited to 1° through programming, although the multiScan is capable of achieving a resolution of 0.5°. This decision was made considering the processing limitations of the PLC used and aiming to keep the data model as lightweight as possible. The entries of the vector are indexed by the azimuth angle θ, with a resolution of 1° per sample, covering the range from $-90°$ to $+90°$. This structured vector is used as input to multiple estimation functions responsible for finding the pallet edges and evaluating geometric offsets.

In the vertical evaluation phase, the sensor is configured to capture measurements from four scan layers, specifically layers 9 to 12, which are evenly spaced by 2.5° in elevation, resulting in a total vertical angular range of 7.5°. Each of these layers provides a single distance measurement.

The vertical data model is therefore defined as a vector of four integer values, each representing a distance in millimeters acquired from one of the selected layers. This corresponds to an angular resolution of 2.5°, which in this case is the maximum resolution supported by the multiScan for vertical scanning. This vector is subsequently used by the vertical offset estimation function to assess the vertical alignment of the pallet.

Together, the horizontal and vertical data models constitute the core inputs to the estimation logic, ensuring that all relevant spatial features of the pallet are represented in a structured and computationally efficient form.

3.3.3 Estimation of pallet's edges position

The basis for detecting and measuring various features on the pallet begins with identifying the positions of its two outer edges (the left and right boundaries).

It is important to note that this function and all others, except for vertical offset estimation and structural fault detection, operates on data acquired from the horizontal scan layer (layer 3).

The process of edge detection involves scanning through the distance vector and searching for values that fall within a certain radius, which are considered to correspond to pallet points. Based on the typical warehouse layout and the minimum possible distances between the pallet and neighboring elements, it is known that the pallet edges will fall within a specific range. This range is referred to as the ***bounding radius,*** as illustrated in Figure 3.15, and it accounts for potential offsets of the pallet.

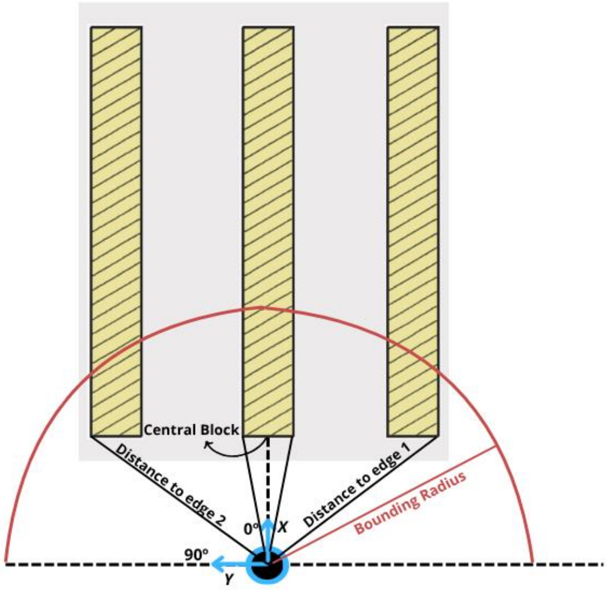

Figure 3.15 - Estimation of pallet's edges position strategy (top view)

If the pallet edges are not found within this radius, it may indicate that no pallet is present or that there is a significant position offset, in which case the program flags an error. Otherwise, the edge's position detection procedure begins by scanning the distance vector from the smallest to the largest azimuth angle (i.e., incrementing the index), where the first value found within the bounding radius is considered the distance from the multiScan to the right pallet edge. After that, the vector is scanned in reverse order, i.e., from the highest index to the lowest, to locate the left pallet edge, again by identifying the first valid distance within the bounding radius.

To ensure that these detected values are not outliers caused by measurement noise, a validation step is applied. The algorithm compares each identified edge distance with its adjacent values, which should also correspond to pallet points and therefore present similar distances. If the detected value deviates significantly from its neighbors, it is considered unreliable, and the search continues until a consistent value is found.

3.3.4 Pallet horizontal offset estimation

Having found the two radial distances to the pallet edges, the horizontal offset is evaluated by computing the y-projection, as illustrated in Figure 3.16, where the lighter-colored pallet represents the reference position. The resulting value is then compared to a reference position, p_R, as shown in Equation 3.1. If the resulting offset, Δy (in absolute value), exceeds the clearance between the SRM fork and the pallet tunnel (see Figure 3.12) an excessive offset is detected and flagged. In that case, the calculated offset value is communicated to the SRM so that it can adjust its position accordingly.

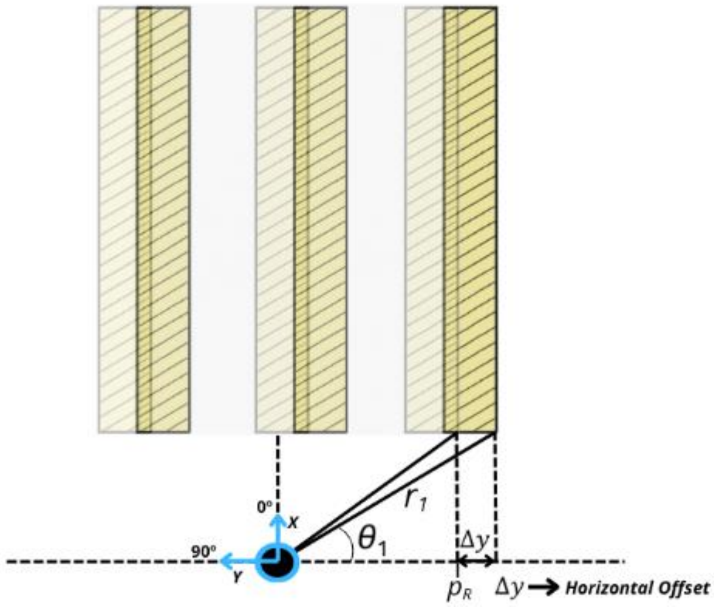

Figure 3.16 - Pallet horizontal offset estimation strategy (top view)

$$\Delta y = r_1 \cos(\theta_1) - p_R \quad (3.1)$$

A threshold was defined for the deviation of the pallet from its reference position beyond which correction by the SRM is no longer permitted. In such cases, the deviation is flagged, but no corrective action is taken by the SRM. When uncorrectable errors or offsets are detected, the SRM is halted, and an operator is notified to assess the situation.

3.3.5 Detection of the pallet’s central block

The algorithm includes a function dedicated to identifying and locating the central block of the pallet, (see Figure 3.15), specifically by detecting its edges. The primary objective is to provide an additional confirmation of the pallet’s presence by verifying whether this block exhibits the expected width, falls within the anticipated angular range, and lies at an appropriate distance from the multiScan, as suggested in Figure 3.17. Furthermore, this function is crucial for determining the azimuth angle at which a vertical plane will be constructed, enabling subsequent analysis of vertical position offsets.

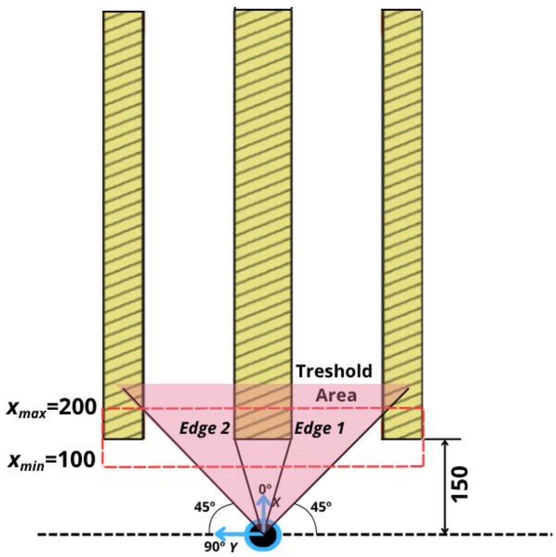

Figure 3.17 - Detection of the pallet's central block strategy (top view)

To identify the edges of the central block, the same strategy used for detecting the outer edges of the pallet is applied, but with a reduced bounding radius and a narrower angular search range.

Once both edges are detected, the algorithm estimates the perpendicular distance (x direction) between the block and the multiScan by sampling values between the detected edges. It then verifies whether this distance falls within the predefined tolerance for possible x-offsets of the pallet. Following this, the y-projections of the edges are computed to determine the block's width, which is then compared against the expected value. This verification allows the system to confirm the presence of the pallet with greater confidence, as the central block is a distinctive structural feature.

3.3.6 Pallet rotational offset estimation

The strategy defined for measuring pallet rotations is based on first computing the difference between the x-projections of r_1 and r_2 (Δx), as illustrated in Figure 3.18.

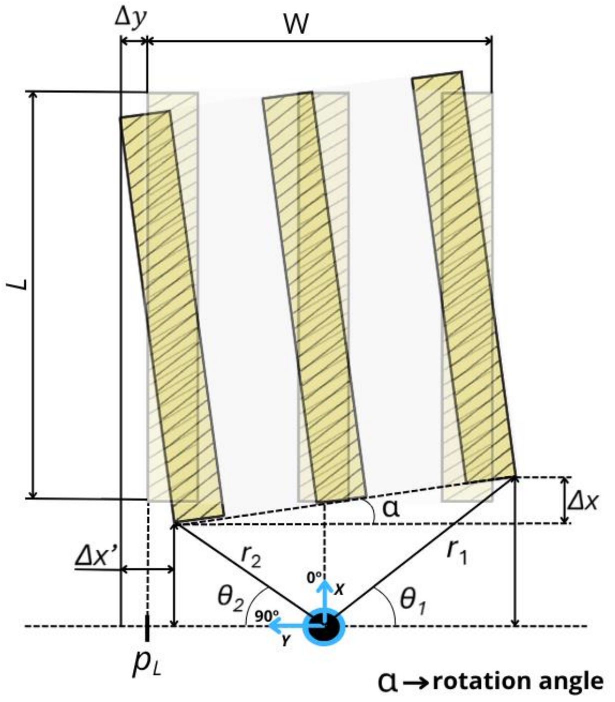

Figure 3.18 - Pallet rotational offset estimation strategy (top view)

The computation of Δx is carried out as shown in Equation 3.2.

$$\Delta x = r_1 \sin{(\theta_1)} - r_2 \sin{(\theta_2)} \tag{3.2}$$

Next, $\Delta x'$ is calculated, which, as illustrated in Figure 3.18, represents the offset generated along the length of the pallet (in the y-direction) due to rotation, and is determined as shown in Equation 3.3.

$$\Delta x' = \frac{L}{W} \Delta x \tag{3.3}$$

Finally, the key value to be determined is Δy, which represents the offset in the y-direction caused by the pallet's rotation, relative to the reference position p_L (see Figure 3.18), as defined in Equation 3.4. In other words, it quantifies how much the pallet has shifted in y with respect to the reference, in order to assess the risk of collision with the SRM fork. To avoid collision, Δy must remain below the clearance between the fork and the pallet tunnel.

$$\Delta y = (r_2 \cos(\theta_2)\ -\ \Delta x') - p_L \tag{3.4}$$

If the absolute value of the calculated Δy exceeds the defined tolerance, the error is flagged, the pallet is identified as rotated, and no autonomous correction can be performed by the SRM. In such cases, operator intervention is required to properly assess the situation and reposition the pallet accordingly.

3.3.7 Pallet vertical offset estimation

To verify whether the relative positioning between the SRM and the pallet in terms of height (*z*-coordinate) is correct and, if not, to quantify the vertical offset, the strategy developed is illustrated in Figure 3.19.

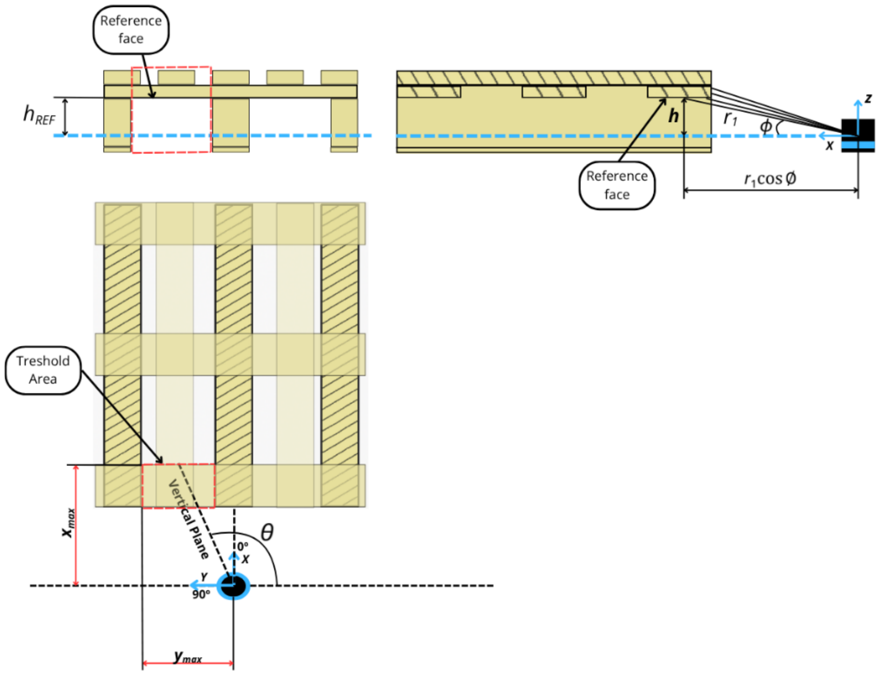

Figure 3.19 - Pallet vertical offset estimation strategy (front, top and side views)

The objective is to measure the vertical distance between layer 3 (the horizontal layer) and the lower face of the upper pallet board, as indicated in the Figure 3.19. Once the positions of the central block's edges are identified, an azimuth angle θ is defined by adding 10° to the angle corresponding to the left edge of the block. This angle is used to define the vertical plane for analysis, composed of multiple scan layers, and ensures that the plane intersects the pallet tunnel and captures the reference face as intended.

It was defined that only four scan layers (excluding the horizontal one) are received from the multiScan to perform this analysis. These are layers 9, 10, 11, and 12, selected based on preliminary tests which confirmed that, when the pallet is in its reference position, these layers intersect the target face while still allowing some margin for positional errors.

As illustrated in Figure 3.19, one of these four layers is expected to project a beam that intersects the target surface. Therefore, the task is to determine which of the four distance values corresponds to that intersection. This is achieved by filtering the values using the threshold area shown in Figure 3.19. If a distance value falls outside this area, it is discarded (set to zero). Inequalities 3.5 and 3.6 describe the filtering criteria used in this process.

$$r_1 \cos(\Phi) \cos(\theta) < y_{MAX} \tag{3.5}$$

$$r_1 \cos(\Phi) \sin(\theta) < x_{MAX} \tag{3.6}$$

For the values that remain different from zero after filtering, their projection along the z-axis (denoted as h) is computed, as illustrated in Figure 3.19 and described in Equation 3.7. These height values may correspond either to points on the target surface or to points located on the front face of the pallet, which is higher than the intended reference surface. Therefore, the value of interest is the lowest non-zero height, as it most likely represents a point on the desired reference face.

$$h = r_1 sin\,(\Phi) \tag{3.7}$$

Finally, the last step consists of subtracting the measured value h from the reference height h_{REF} which represents the expected vertical distance between the pallet face and the horizontal scan layer of the multiScan. This subtraction yields the estimated vertical offset Δz, as expressed in Equation 3.8.

$$h_{REF} - h = \Delta z \tag{3.8}$$

3.3.8 Pallet structural faults detection

Lastly, the detection of potential structural faults, such as broken blocks, loose wood fragments, among others, is supported by the multiScan's integrated Field Evaluation function, previously described in an earlier section.

The strategy consists of defining two evaluation fields aligned with the two fork arms of the SRM, with dimensions approximately matching those of the fork elements. If either field is obstructed by an object, a digital output from the multiScan is activated, signaling that there is an obstacle in the fork's path which may lead to a collision. This obstacle could be a protruding structural fault, such as a displaced broken component, or even the pallet itself if it is misaligned and its tunnels are not properly positioned. In this sense, the function also acts as a validation mechanism for the results obtained from the preceding estimation functions. Figure 3.20 shows, via SOPAS Air, the two evaluation fields created and positioned within the pallet tunnels used for testing.

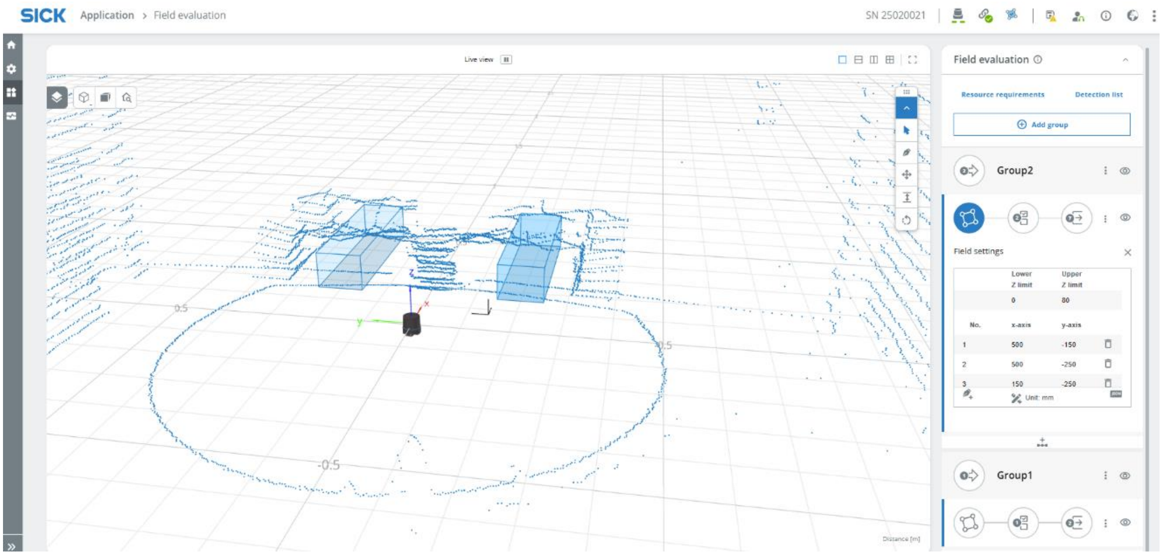

Figure 3.20 - Field evaluation implemented on SOPAS Air

However, this approach has certain limitations. As previously explained and shown in Table 3.2, the Field Evaluation function has minimum detection dimensions. Given the typical distance between the multiScan and the pallet, the minimum detectable object width is around 13 mm, and the height around 20 mm. This implies that small fragments, such as thin splinters of wood that could still cause a collision or a pallet drop, may not be detected, as they fall below the resolution threshold of the sensor.

A second limitation relates to the positioning of the multiScan, since it is mounted centrally relative to the pallet, it cannot fully observe the depth of the pallet tunnels due to occlusion effects. The sensor generates shadow zones and can only scan up to a limited depth, as represented in Figure 3.21. Two main strategies can be considered to overcome this constraint: either using two multiScan sensors, each targeting one tunnel, or making the SRM perform a lateral shift to allow a complete scan of both tunnels. The main drawbacks of these alternatives are increased system cost in the first case, and reduced cycle time in the second.

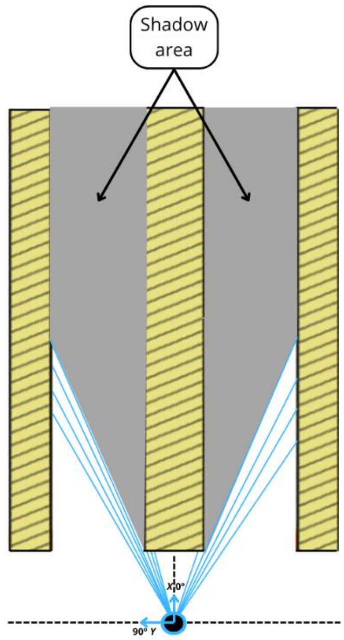

Figure 3.21 - MultiScan shadow area (top view)

3.4 Summary

This chapter presented the key components involved in the development of the pallet evaluation solution. It began with an overview of the selected LiDAR sensor, the SICK multiScan165, including its measurement principles, coordinate system, filtering capabilities, and data output format. These characteristics provided the foundation for understanding the type and structure of data available for further processing.

Subsequently, the chapter detailed the algorithms developed for assessing the pallet's position and structural integrity. The operational data model was defined to prepare the input used by the estimation functions. These functions were then described, including the detection of the pallet's edges and central block, as well as the estimation of horizontal, rotational, and vertical offsets. Finally, a structural fault detection stage was introduced to ensure the overall reliability of the evaluation.

The following chapter focuses on the implementation of the developed system within the Siemens S7-1200 PLC environment. It presents the main components of the control logic, describes the program structure and execution flow, and details the communication setup with multiScan. Additionally, it explains how the measurement data is acquired, pre-processed, and prepared for subsequent feature estimation tasks within the PLC.

4 Integration with Siemens S7-1200 PLC

This chapter presents the integration of the developed solution with the Siemens S7-1200 PLC. It begins by introducing the selected PLC and the overall program structure. The communication between the PLC and the multiScan is then detailed. Finally, the chapter describes the data acquisition and pre-processing routines implemented in the PLC, which prepare the sensor's data model for the estimation functions.

4.1 The S7-1200 PLC

The SIMATIC S7-1200, shown in Figure 4.1, is a compact and scalable PLC developed by Siemens, designed for automation tasks in the low to medium performance range. It integrates digital and analog inputs/outputs, communication interfaces, and a set of built-in technology functions such as high-speed counting, pulse-width modulation, and positioning control. Its modular architecture allows flexible expansion through additional I/O and communication modules, making it suitable for a wide range of industrial applications [14].

Figure 4.1 - SIMATIC S7-1200

The specific PLC model used during the project was the SIMATIC S7-1200 PLC, CPU 1214C. This controller features a PROFINET interface via RJ45 Ethernet and includes 75 KB of work memory and 4 MB of load memory. It was the unit made available for testing and program development throughout the project [15].

Given that the S7-1200 is a low-performance class PLC, it was necessary to adopt an efficient programming strategy for data handling, as this type of controller is not designed for point cloud processing, which involves large volumes of data. The limited availability of built-in libraries for such tasks further increased the programming effort required.

The SRMs, however, operate with S7-1500 series PLCs, which are engineered for more complex applications requiring higher computational performance. These controllers offer significantly greater processing power. Nevertheless, access to an S7-1500 was only possible in the later stages of the project.

TIA Portal (Totally Integrated Automation Portal) is Siemens' integrated engineering environment used for configuring, programming, and testing automation systems such as PLCs, HMIs, and drives. It provides a unified platform that simplifies the entire development workflow, from hardware setup to real-time diagnostics. The programming environment is illustrated in Figure 4.2.

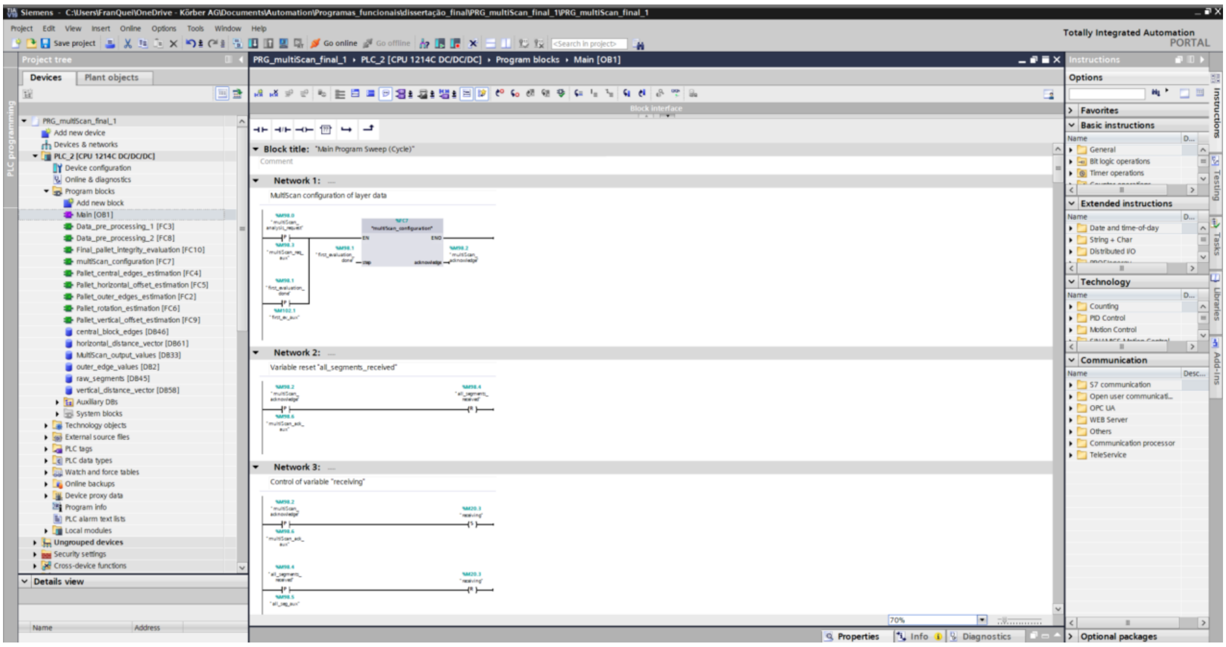

Figure 4.2 - TIA Portal environment

All programming and testing activities in this project were carried out within TIA Portal, making it the central environment for developing and validating the PLC logic. The software supports various languages, including Ladder Logic (LAD), Function Block Diagram (FBD), Structured Control Language (SCL), and Statement List (STL). In this application, LAD was primarily used in the main program to organize the sequencing of core functions, while SCL was chosen for implementing the internal logic of the functions due to its greater flexibility.

4.2 Program structure and execution flow

This section provides an overview of the program structure and the logical flow of execution within the PLC. Figure 4.3 to Figure 4.6 present the program logic of the main routine, structured to illustrate the high-level stages of the algorithm. The sequence highlights the overall execution flow, from the initial triggering of the multiScan data analysis to the final evaluation of the pallet condition.

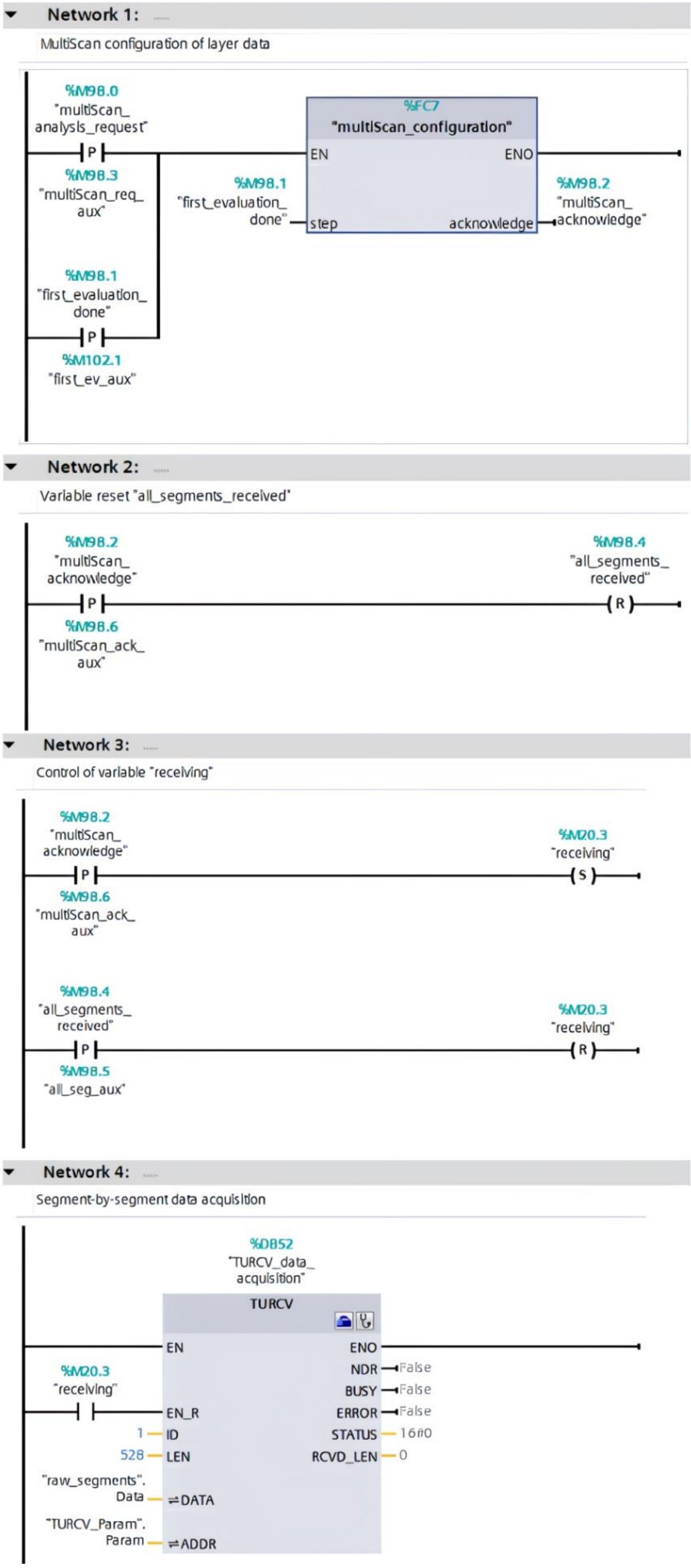

Figure 4.3 - Program logic – networks 1 to 4

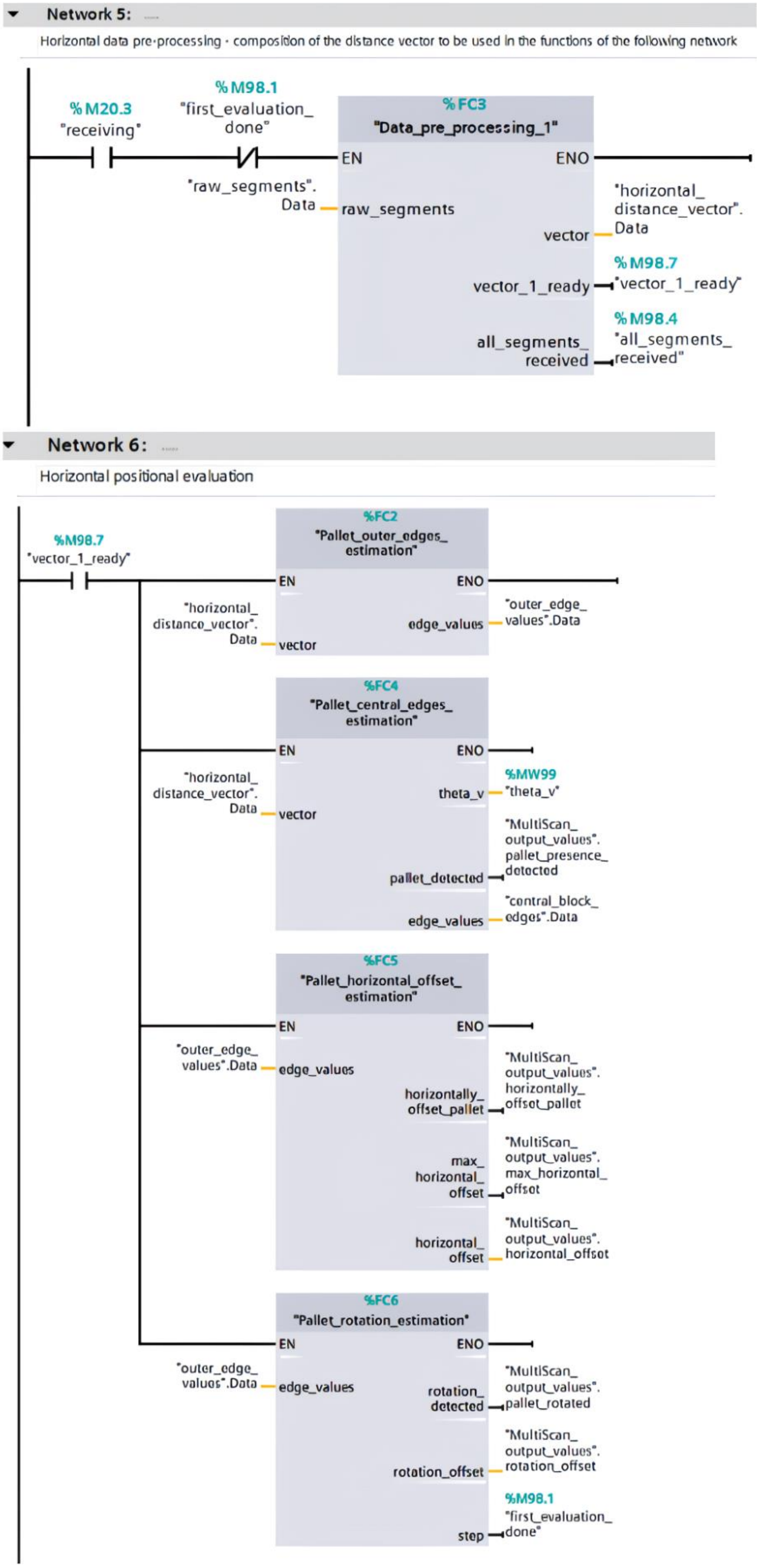

Figure 4.4 - Program logic – networks 5 and 6

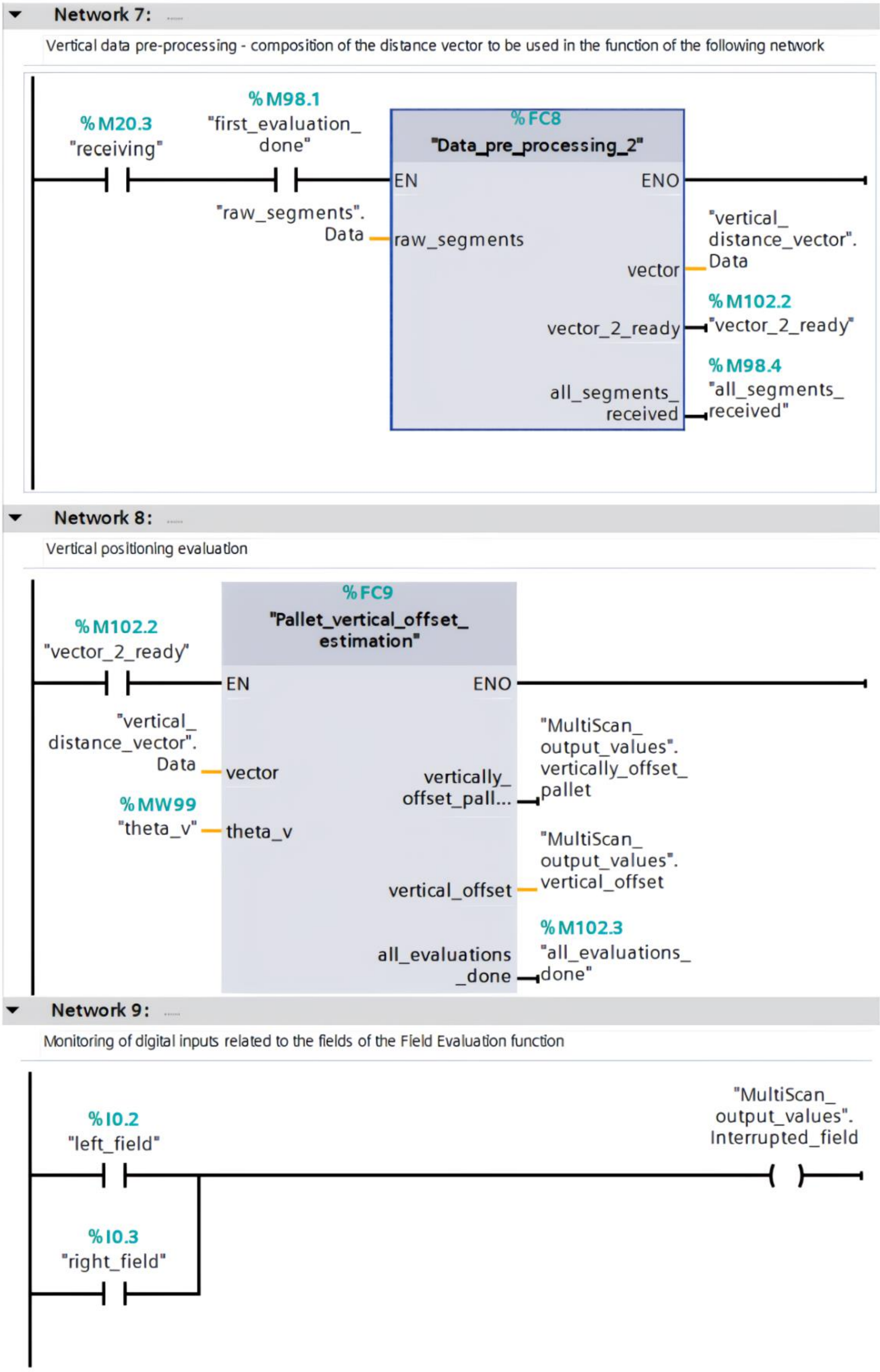

Figure 4.5 - Program logic – networks 7 to 9

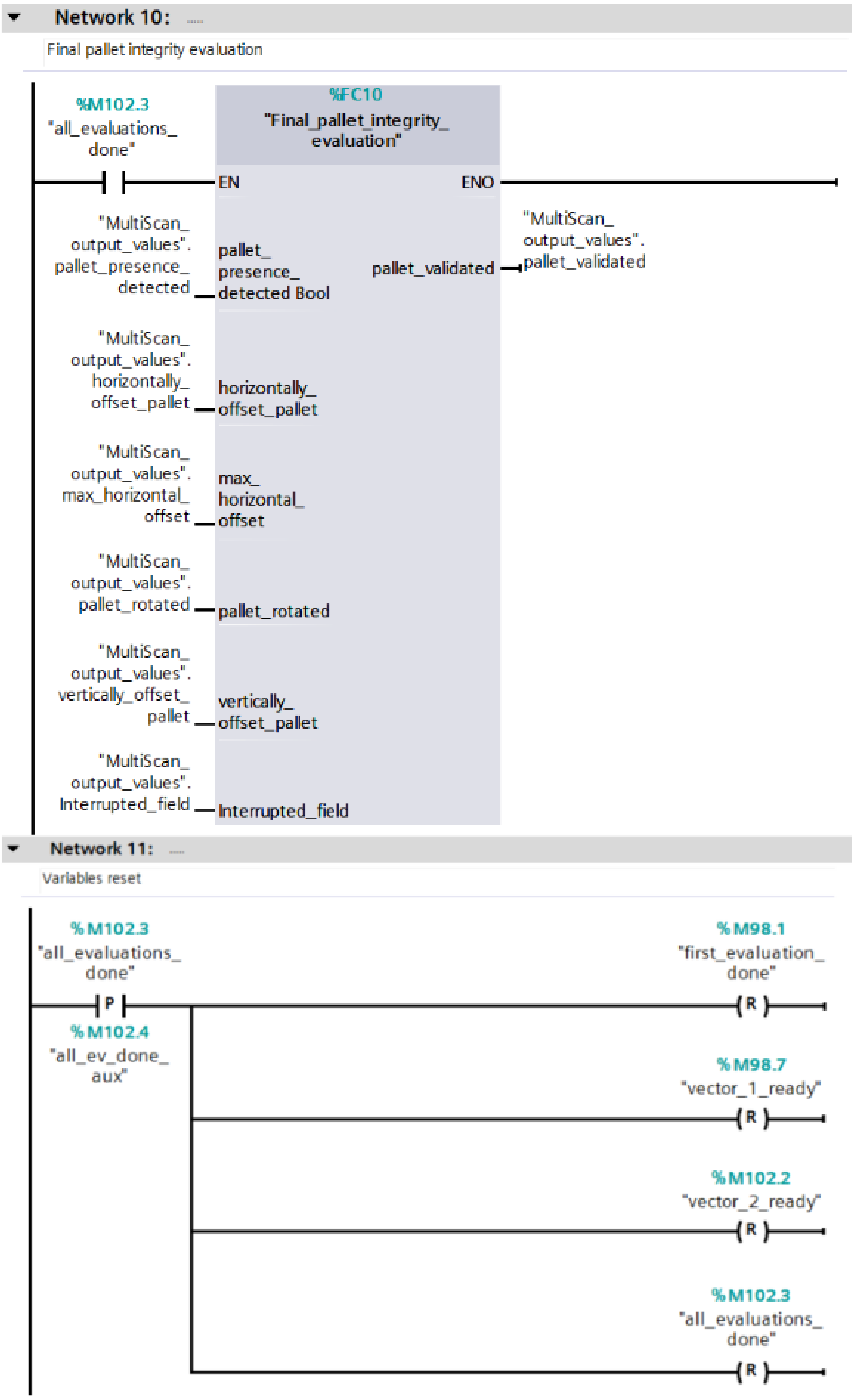

Figure 4.6 - Program logic – networks 10 and 11

The program logic is structured into two main phases: horizontal evaluation and vertical evaluation. Each phase encompasses sensor configuration, data acquisition, and processing steps, culminating in a final decision regarding pallet acceptance.

In the network 1, the program remains in a standby state until a trigger request initiates the multiScan analysis. Once triggered, the multiScan sensor is configured to acquire data from the horizontal layer, which provides a planar profile of the pallet. The data is collected segment by segment (network 4) and passed through a pre-processing routine (FC3, `Data_pre_processing_1`) that extracts and organizes the relevant information, present in network 5. This results in a distance vector composed of 180 integers, indexed by azimuth angle θ over a 180° range. Based on this vector, a series of evaluation functions are executed, in network 6, to estimate the pallet's outer edges (FC2), detect the central block (FC4), and assess both horizontal and rotational offsets (FC5 and FC6).

The second phase focuses on evaluating the pallet's vertical condition. This involves activating multiple scan layers positioned at different heights and acquiring their respective data (network 1 and 4, respectively). The measurements are sequentially processed through a second pre-processing function (FC8), present in network 7, producing a vertical distance vector of four integers, each corresponding to a specific scan layer. This vector serves as input to FC9 (`Pallet_vertical_offset_estimation`), which assesses the pallet's vertical alignment (network 8).

Finally, all extracted features—together with the status of two digital inputs related to the Field Evaluation function (present in network 9)—are combined in a final decision-making routine that performs the Pallet Integrity Evaluation, determining whether the pallet satisfies the required geometric and structural conditions for automated handling (network 10).

In Figure 4.7 and 4.8, an example of the programming of one of the FCs is shown, specifically FC5, `Pallet_horizontal_offset_estimation`, which was implemented in SCL. This FC was implemented following the methodology described in Section 3 concerning the strategy for estimating the horizontal offset. It receives as input the variable `edge_values`, which is an array of four integers corresponding to the distances to the two outer pallet edges and their respective azimuth angles. More precisely, the first element of the array stores the distance to the right edge, r_1 (as illustrated in Figure 3.16), the second element holds its corresponding angle θ_1, the third stores the distance to the left edge, and the fourth holds its respective angle.

The FC first converts the angle θ_1, retrieved from `edge_values[2]`, into radians and assigns it to the variable `theta_1`. It then computes the y-projection of r_1 (stored in `edge_values[1]`), which is represented by the real variable `y1`, following equation 3.1. Subsequently, the horizontal offset Δy is calculated as the difference between `y1` and the reference position `P_R`, and the result is assigned to the variable `horizontal_offset`.

If this calculated offset exceeds the defined tolerance but remains below the maximum allowable offset (`max_offset`), the Boolean output `horizontally_offset_pallet` is set to TRUE, indicating the presence of a correctable horizontal pallet offset. Conversely, if the offset surpasses `max_offset`, the output `max_horizontal_offset` is set to TRUE, signifying that the maximum horizontal deviation has been reached and it is not feasible to adjust the SRM position automatically. If the offset stays within the acceptable tolerance, both Boolean outputs (`horizontally_offset_pallet` and `max_horizontal_offset`) remain FALSE, indicating that the pallet is properly positioned within the allowable limits.

Pallet_horizontal_offset_estimation

	Name	Data type	Default va..	Comment
1	Input			
2	edge_values	Array[1..4] of Int		
3	edge_values[1]	Int		
4	edge_values[2]	Int		
5	edge_values[3]	Int		
6	edge_values[4]	Int		
7	Output			
8	horizontally_offset_pallet	Bool		
9	max_horizontal_offset	Bool		
10	horizontal_offset	Int		delta_y
11	InOut			
12	Temp			
13	y1	Real		y projection
14	theta_1	Real		theta_1 in radians
15	Constant			
16	tolerance	Int	50	
17	P_R	Int	400	
18	PI	Real	3.141593	
19	max_offset	Int	70	

Figure 4.7 - FC5 variables

Network 1: .....

FC5 Pallet_horizontal_offset_estimation

```
#theta_1 := (#edge_values[2]) * (#PI / 180);
#y1 := #edge_values[1] * COS(#theta_1);

#horizontal_offset := ROUND(#y1 - #P_R);

IF ABS(#horizontal_offset) > #tolerance AND ABS(#horizontal_offset) < #max_offset THEN
    #horizontally_offset_pallet := TRUE;
    #max_horizontal_offset := FALSE;

ELSIF ABS(#horizontal_offset) > #max_offset THEN
    #max_horizontal_offset := TRUE;
ELSE
    #horizontally_offset_pallet := FALSE;
    #max_horizontal_offset := FALSE;
END_IF;
```

Figure 4.8 - Programming of the FC5 `Pallet_horizontal_offset_estimation`

4.3 Communication between PLC and the multiScan

In order to effectively integrate the multiScan with the Siemens S7-1200 PLC, two types of communication were established: UDP (User Datagram Protocol), where the PLC listens for measurement data sent by the sensor on port 2115, and TCP (Transmission Control Protocol), where the PLC sends commands to the multiScan to modify specific configurations. This phase ensured that the multiScan could be operated and queried autonomously by the PLC, eliminating the need for external software.

The communication between the devices is established using Siemens “Open User Communication” (OUC) library, which provides standardized function blocks (FBs) for managing network communication within the SIMATIC S7 environment. This library facilitates the setup, maintenance, and termination of communication sessions over Ethernet networks, supporting protocols such as TCP and UDP. By utilizing the OUC library, the integration process is simplified by abstracting the complexities of the underlying network protocols, enabling the PLC program to manage communication more efficiently. The following subsections will describe several FBs that are part of this library.

4.3.1 Configuration of the UDP communication

The initial setup to establish a UDP communication utilizes the TCON and TDISCON FBs, as shown in Figure 4.9. The TCON FB is responsible for establishing and managing the communication connection to the external device over the UDP protocol. It opens the socket and maintains the session parameters throughout operation. The complementary TDISCON FB is used to properly close the communication channel when it is no longer required, ensuring a clean and orderly shutdown of the connection [16].

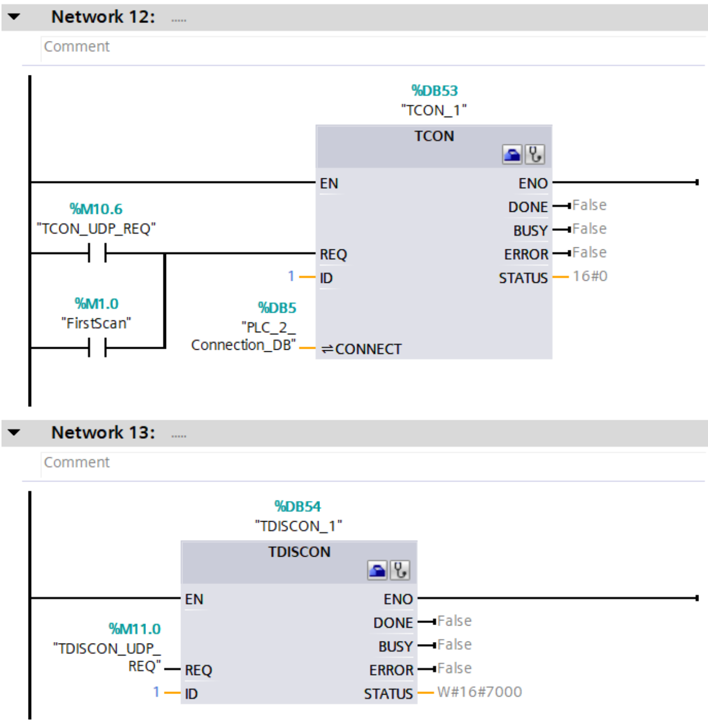

Figure 4.9 - TCON and TDISCON FBs in TIA Portal environment

For the communication to function correctly, network parameters must be precisely configured. The Ethernet interface of the Siemens PLC is assigned a static IP V4.0 address, here set to 192.168.0.10, which must reside within the same subnet as the multiScan to enable proper routing of UDP packets. Additionally, the PLC is configured to listen on a specific local UDP port - in this case, port 2115 - which corresponds to the port the multiScan sensor transmits its measurement telegrams to. The sensor itself is configured accordingly to send its UDP data packets to the PLC's IP address and listening port.

Within the TCON FB, several key parameters are specified to define the connection's properties, as presented in Figure 4.10. The connection type is set to UDP, indicating the use of a connectionless datagram protocol that suits real-time streaming requirements. A connection ID, set to 1, uniquely identifies this communication channel within the PLC program. The block also references a connection data block (DB), which stores parameters such as the remote IP address, remote port, local port, among others, consolidating configuration details in a structured manner. In this case, because it's a UDP connection, specifying the remote IP address and remote port is not required, only the local port, which is set to 2115 [16].

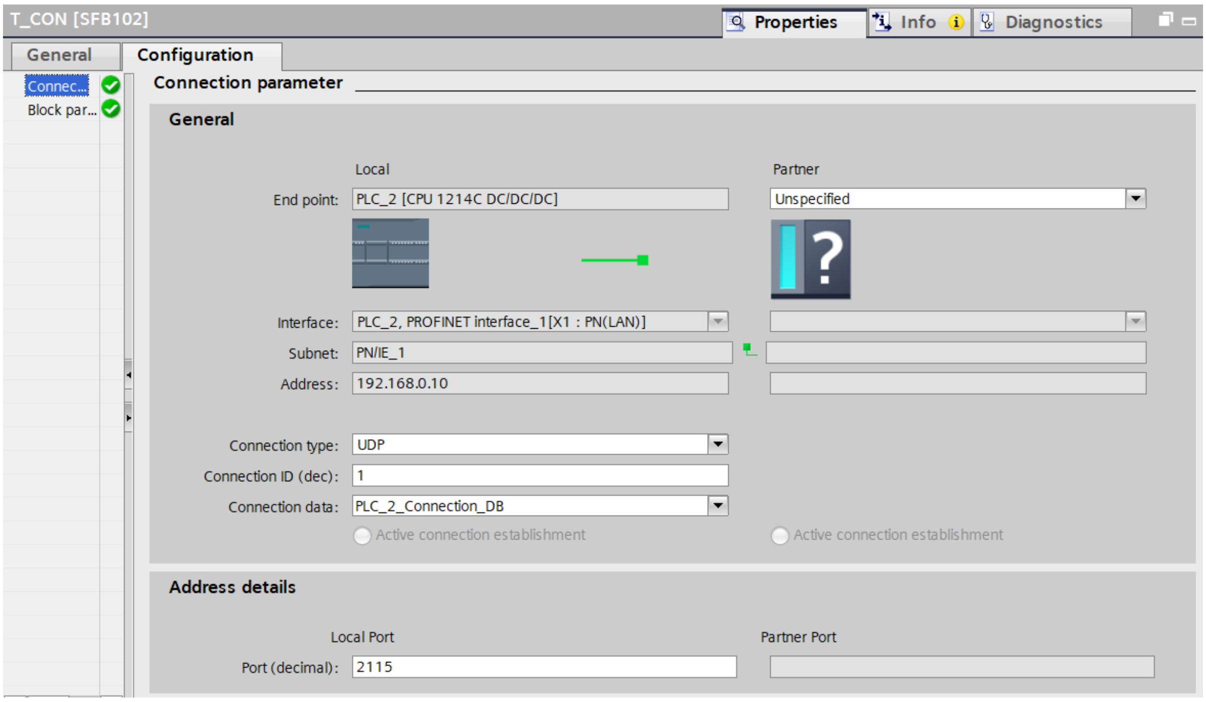

Figure 4.10 - TCON, connection parameters specification

Once the connection is established and managed by TCON, incoming measurement data is received using the TURCV FB, as illustrated in Figure 4.11. This block listens for UDP telegrams on the specified socket and transfers the received data into a designated data buffer within a DB. The reception process is controlled by the enable receive trigger (EN_R), which activates the TURCV FB to receive incoming packets. The connection ID used in TURCV matches that of the TCON block to ensure data is received from the correct source. The LEN parameter defines the expected size in bytes of each UDP telegram, which must correspond to the size of the multiScan data format selected. The data is stored in a preconfigured DB, such as `raw_segments`, within its DATA field [16].

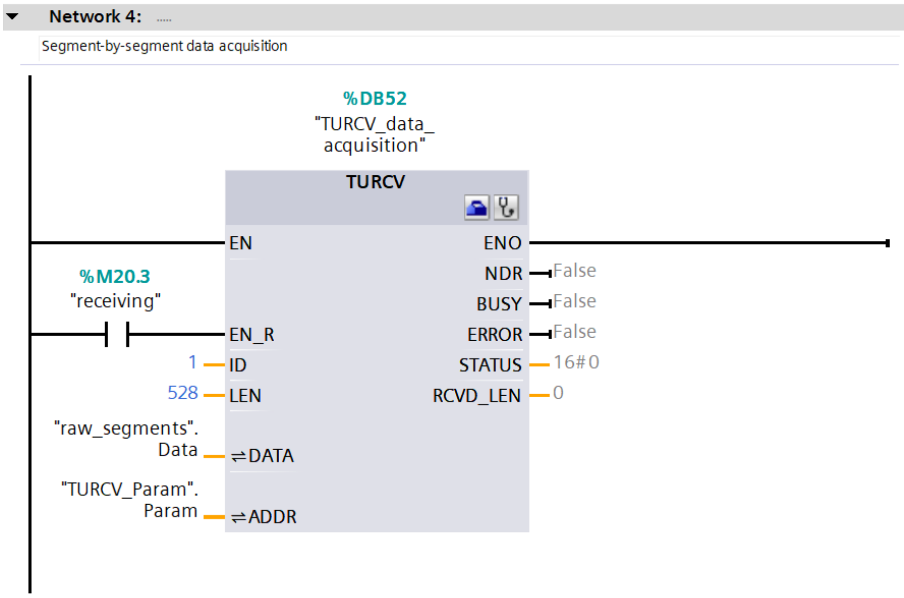

Figure 4.11 - TURCV FB

This configuration enables the PLC to reliably receive and buffer multiScan measurement data in real time, making it accessible for subsequent decoding and analysis within the control program.

4.3.2 Configuration of the TCP communication

The TCP is used to send commands from the PLC to the multiScan sensor, specifically to modify certain configurations necessary for its intended functionality. As explained below, these commands primarily aim to alter the layer filters, that is, determining which layers are active or inactive at any given moment.

It is important to note that a predefined configuration where all layers are always active and the PLC simply filters the necessary layers was not feasible due to the limitations of the Siemens S7-1200 PLC. This PLC cannot receive UDP packets larger than 1472 bytes through the TURCV FB. Given the configuration in place on the multiScan, with the intention of receiving only the last echo, each UDP packet for a single layer is 528 bytes. Therefore, it is not possible to receive more than two layers per packet. As a result, the chosen solution was to modify the layer filters dynamically, sending commands to the multiScan to activate or deactivate specific layers as required by the PLC during operation [16].

In this case, TCP was chosen for sending commands to the multiScan, as it is crucial to ensure that each configuration change is applied correctly and confirmed by the device. This ensures the proper functioning of the system. The commands are sent using the CoLa A protocol, which is an ASCII-based communication protocol.

The three commands that were used throughout the program execution are shown in Table 4.1.

Table 4.1 - Commands sent to the multiScan via CoLa A protocol

Command	Command Format (ASCII)
Log in	$02sMN SetAccessMode 03 F4724744$03
Set Layer Filter	$02sWN LFPlayerFilter 1 0 0 1 0 0 0 0 0 0 0 0 0 0 0 0 0$03
Log out	$02sMN Run$03

The first step is to log in to the multiScan using the log in command. This command authenticates the PLC with the sensor, allowing it to modify parameters [17].

The second command (Set Layer Filter Command) is used to configure the layer filter. For example, the command present in Table 4.1 activates the filter by disabling all layers and enabling only the horizontal layer (layer 3). In this command, the first "1" indicates activation of the filter, and the subsequent "0" or "1" values represent the state of each of the 16 layers in sequence, where "1" means active and "0" means inactive [17].

At last, once the required configuration is made, the final step is to log out from the device to finalize the changes with the third command, which finalizes the session, making all the changes active and ensuring the system operates with the updated configuration [17].

The FBs required to send commands and receive confirmation responses from the multiScan are TSEND_C FB and TRCV_C FB, respectively. These FBs also belong to the OUC library but differ from the previously mentioned blocks (TCON, TDISCON, and TURCV) in that they combine the functions of establishing, maintaining, managing, and terminating the connection, previously handled by TCON and TDISCON, while also incorporating the capability to send data (TSEND_C) and receive data (TRCV_C) [16].

In Figure 4.12, the configuration of the TSEND_C parameters is shown. In this case, the connection type is set to TCP, and the connection ID must differ from the one used for the UDP connection, here, it is set to ID 2. The PLC is configured as the active element in the communication, acting as the client. The partner port is set to 2111, a predefined port used for receiving CoLa A commands over TCP. The configuration for the TRCV_C FB is similar, as it refers to the same connection where the PLC continues to act as the client, but now it simply receives the response from the server, in this case, the multiScan [16].

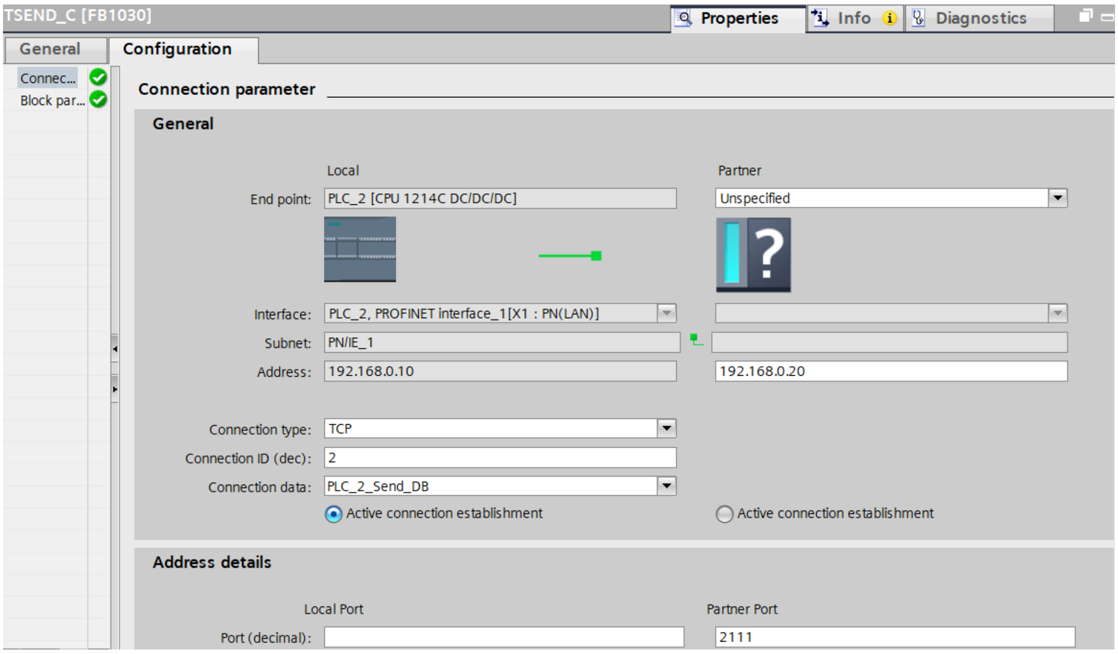

Figure 4.12 - TSEND_C, connection parameters specification

In Figure 4.13, the two FBs can be observed. Among the parameters displayed, the REQ parameter in TSEND_C is particularly noteworthy, as it starts the sending process on a rising edge. Additionally, in TSEND_C, the Data parameter is linked to a DB that contains the command to be sent (`Send_command`). In TRCV_C, the Data parameter is where the responses from the multiScan are received. Finally, the DONE output parameter is set to TRUE whenever data is successfully received by the block. This parameter plays a critical role in the programming, as it serves as confirmation that the sensor's response has been successfully received [16].

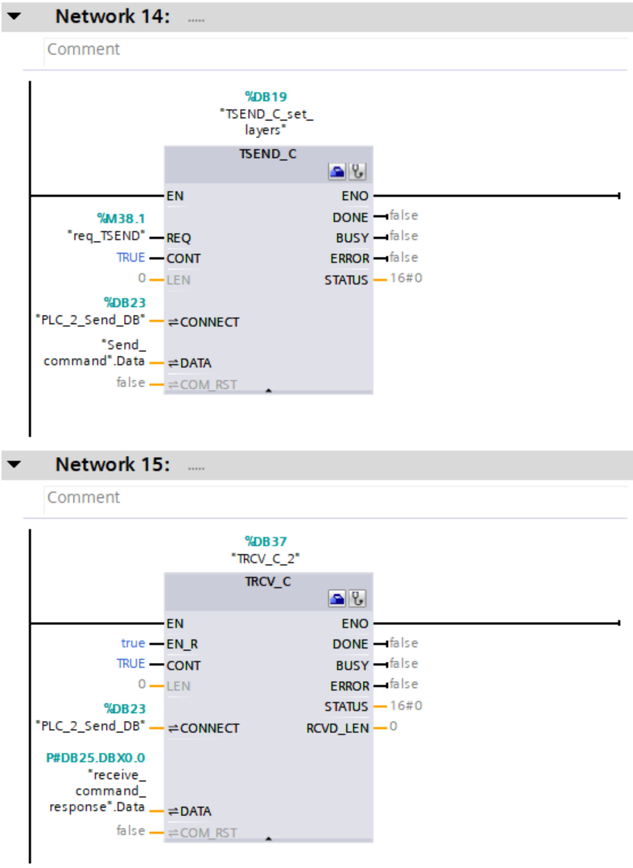

Figure 4.13 - TSEND_C and TRCV_C FBs

4.4 Data acquisition and pre-processing programming

This stage focused on implementing a robust data acquisition pipeline inside the PLC. The raw data received from the sensor was structured into appropriate memory blocks (DBs), decoded, and filtered to retain only the most relevant information. The main goal of this pre-processing step is to construct a distance vector, where each index corresponds to a specific azimuth angle and holds the respective measured distance in millimeters, restricted to a desired angular range.

It is important to emphasize that the analysis is performed layer by layer, as each layer corresponds to a distinct elevation angle (ϕ) in the sensor's multi-layer scan. For a given layer, the multiScan provides a radial distance measurement for each azimuth angle, effectively generating a distance map.

In the case of the horizontal layer, each data point is defined in polar coordinates, with a radial distance measured for each azimuth angle. For layers with non-zero elevation angles, the measurements are naturally represented in spherical coordinates, as each beam is characterized by both azimuth and elevation angles along with its radial distance.

As explained in the previous section, once the TURCV FB is activated to receive data, the multiScan sensor continuously sends measurement telegrams at a frequency of approximately 10 Hz (this may vary depending on the active filters). The first step in the pre-processing routine is to read the segment counter filed from each incoming telegram. This value, located at byte position 33, uniquely identifies which portion of the 360° scan the telegram corresponds to. As previously discussed, each segment represents a fixed 30° portion of the full

360° scan. For example, segment 3 consistently corresponds to the angular interval [-90°, -60°] (Figure 3.9).

To facilitate further processing, the system allocates a dedicated buffer for each of the 12 possible segments. Upon reception, each telegram is routed to its corresponding buffer based on the segment counter value. For instance, a telegram with segment number 1 is stored in the buffer assigned to segment 1, segment number 2 in buffer 2, and so on.

This structured allocation ensures that all relevant segment data can be easily accessed and reassembled later into a complete and ordered frame.

The next step involves performing the frame assembly for the desired angular range and extracting from each segment telegram only the payload, that is, the distance values.

Assuming the goal is to construct a distance map for a single layer (for example, the horizontal one) over an azimuth range of 180°, the process begins by selecting and storing the relevant segment telegrams that cover this angular span, in this case, segments 3 to 8. From each of these segments, only the bytes corresponding to distance measurements are extracted. Each distance is represented by a pair of bytes, and each segment provides distance data over a 30° range. These values are sequentially collected and added into a unified vector, forming a continuous 180° distance map composed of hexadecimal byte pairs.

It is important to note that the angular resolution within each segment telegram is 0.5°, meaning there is one distance value per half-degree of beam angle. However, considering the need to minimize the processing load on the PLC, only one value per full degree is extracted.

The final step in this stage is to convert each pair of hexadecimal bytes into a single decimal integer, representing the measured distance in millimeters. The result is a final vector of 180 elements, each corresponding to a one-degree beam within the 180° field of view.

4.5 Summary

This chapter detailed the implementation of the developed solution on the Siemens S7-1200 PLC. It began by presenting the hardware characteristics of the selected controller, followed by an overview of the program structure and execution logic. The communication interfaces with the SICK multiScan sensor were then described, highlighting the configuration of both UDP for data reception and TCP for command transmission. Finally, the procedures for data acquisition and pre-processing were explained, including the generation of structured input vectors for the feature estimation routines.

The next chapter focuses on the experimental validation of the proposed solution. It presents the test methodology used to assess the program's ability to estimate the intended pallet features and discusses the results obtained, with the aim of evaluating the overall performance of the program and the multiScan sensor.

5 Experimental tests and results validation

This chapter presents the experimental tests conducted to validate the main functions of the proposed solution, along with a description of the corresponding setup. The adopted methodology is detailed, followed by the presentation and analysis of the results for each specific function. Furthermore, one of the final sections offers a global discussion of the results, allowing for an integrated evaluation of the proposed solution. Additionally, a comparison of the program execution times on two different PLCs is also included.

5.1 Experimental setup

Figure 5.1 and Figure 5.2 show the hardware components used during testing.

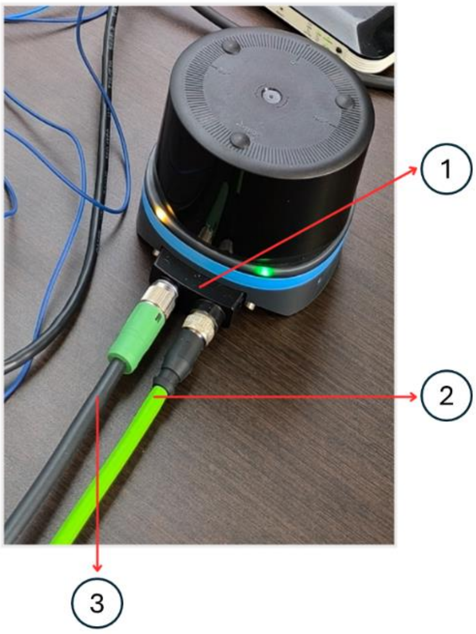

(1) system plug with ethernet connection, 4-pin M12 female connector and power connection, 12-pin M12 male connector.

(2) PROFINET cable, RJ45 to M12.

(3) Power and control cable, M12.

Figure 5.1 - MultiScan system plug and cables

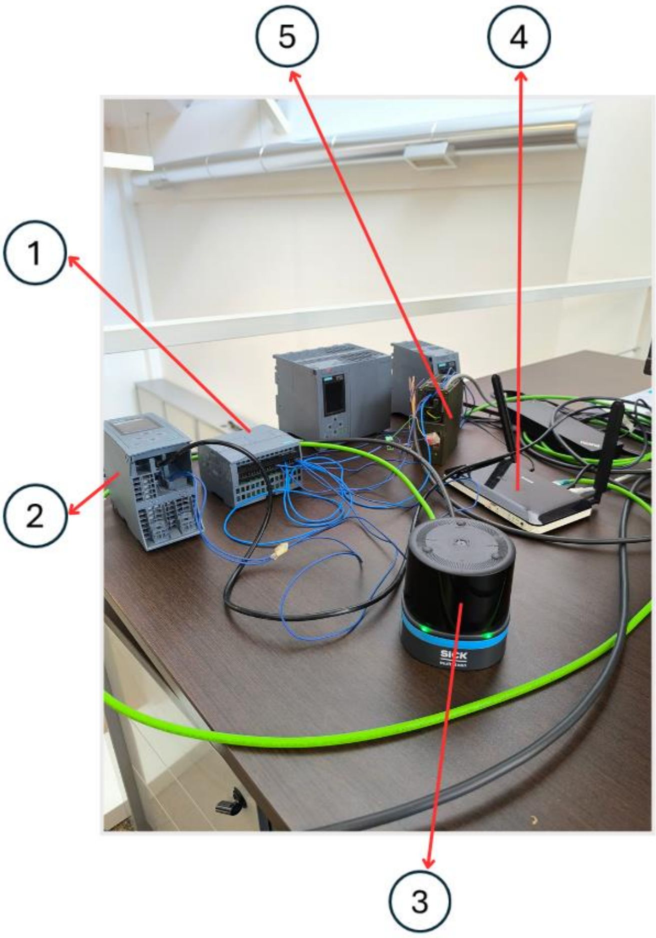

(1) SIMATIC S7-1200 PLC, CPU 1214C.

(2) SIMATIC S7-1500F PLC, CPU 1515F-2 PN.

(3) MultiScan165.

(4) D-LINK DWR-921 Router.

(5) SIMATIC S7-300 Regulated Power Supply PS307.

Figure 5.2 - Hardware setup

It should be noted that, throughout the development phase, the evaluation program was consistently tested and adapted using the S7-1200 PLC. Only during the final test phase was the S7-1500 PLC made available, primarily for the purpose of evaluating the program's execution time and comparing the performance between the two PLCs. All remaining results were obtained using the S7-1200.

Figure 5.3 illustrates the remainder of the experimental setup, which consists of the test pallet placed over a floor duct in the company's office environment. The multiScan was positioned on the floor, aligned with the pallet.

Figure 5.4 and Figure 5.5 illustrate the test pallet dimensions and the relative placement of the multiScan in relation to the pallet.

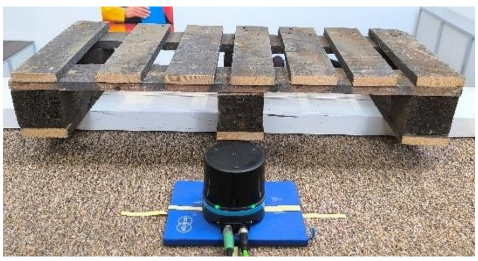

Figure 5.3 - Experimental setup: test pallet and multiScan positioning

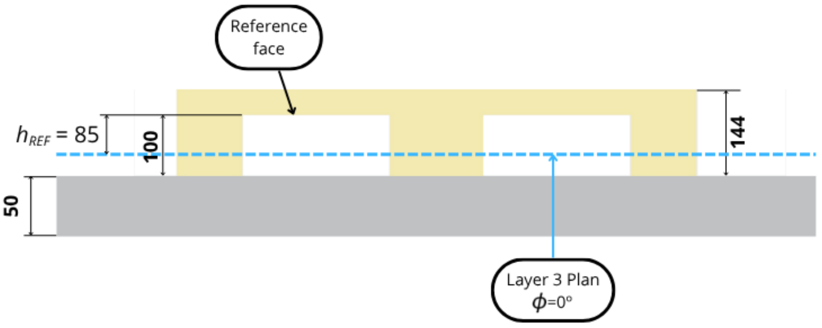

Figure 5.4 - Dimensions of experimental setup, front view

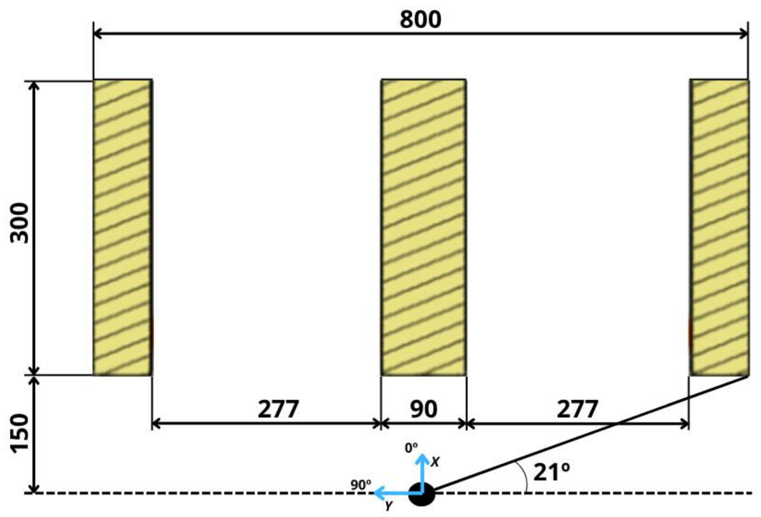

Figure 5.5 - Dimensions of experimental setup, top view

5.2 Test cases and methodology

To evaluate the performance of the developed program, four distinct test cases were defined, each corresponding to one of the key pallet-related features analyzed by the system: horizontal offset, rotation offset, vertical offset, and structural fault detection. Each test case focuses on verifying the system's ability to detect or estimate the respective deviation or condition.

For the horizontal and vertical offset estimation test cases, a set of controlled offset values was introduced in order to observe the program's response across different magnitudes of deviation. Each offset value was tested three times under identical conditions, meaning that other variables, such as vertical offsets or pallet rotations (in the case of horizontal offset test), were kept constant, allowing the analysis to isolate the feature under evaluation. The error between the measured and actual value was calculated for each iteration.

In the case of rotational offset, however, it was not feasible to apply controlled and measurable angular deviations due to limitations in the experimental setup. As a result, this test was carried out qualitatively.

The fourth test case, corresponding to structural faults detection, involved the deliberate introduction of obstructions into the pallet geometry to assess the system's capability to identify anomalies that could compromise proper handling or lead to collisions during SRM operation.

A measuring tape and reference marks were used to perform all required manual measurements.

5.3 Test case 1: Horizontal offset estimation

This section aims to assess the proposed solution for estimating horizontal offsets between the pallet and the reference position. It first introduces the purpose and describes the experimental setup adopted for testing, and then presents the results along with their analysis.

5.3.1 Objective and setup

The main goals of this test case are to validate whether the system is capable of estimating the horizontal offset introduced in the pallet position, and to quantify its accuracy under controlled conditions. To this end, key performance metrics such as the maximum absolute error and the mean absolute error are calculated. These values are then compared against the existing typical clearance between the SRM fork and the pallet tunnel (50 mm) to assess whether the estimation remains within acceptable limits. Additionally, based on the magnitude of the observed errors, a suitable operational tolerance threshold may be proposed to ensure safe and reliable use of the system in a real warehouse environment.

To apply the offsets to the pallet, manual repositioning was carried out. In order to measure the actual offsets introduced, reference markings were made on the floor duct, on both the left and right sides of the pallet, as illustrated in Figure 5.6.

All measurements were conducted with the multiScan positioned at its reference height relative to the pallet, corresponding to 85 mm from the sensor's horizontal layer to the reference face of the pallet, as illustrated in Figure 5.4.

Figure 5.6 - Reference markings on the left side of the pallet

5.3.2 Results and analysis

Table 5.1 presents the test results along with the corresponding errors and key performance metrics.

Table 5.1 - Results of the horizontal offset estimation tests

Horizontal offset estimation						
Test number	Real offset [mm]	Iteration	Measured offset [mm]	Absolute error [mm]	Maximum absolute error [mm]	Mean absolute error [mm]
1.	-50	1	-57	7	10	6
		2	-43	7		
		3	-44	6		
2.	-20	1	-16	4		
		2	-23	3		
		3	-22	2		
3.	0	1	6	6		
		2	4	4		
		3	5	5		
4.	20	1	29	9		
		2	28	8		
		3	30	10		
5.	50	1	57	7		
		2	59	9		
		3	57	7		

The results presented in Table 5.1 demonstrate the system's ability to estimate horizontal offsets applied to the pallet. Across all test cases, the measured offsets show a consistent correlation with the real values introduced. The maximum absolute error observed was 10 mm, while the mean absolute error across all tests was 6 mm.

Considering the real system includes a 50 mm clearance between the SRM fork and each side of the pallet tunnel, and taking into account the maximum measurement error of 10 mm, a tolerance threshold of ±40 mm is proposed. This ensures that even in worst-case conditions, the estimated offset will remain within safe operational bounds.

In conclusion, the system is capable of detecting horizontal offsets with sufficient precision for operational use, and the proposed tolerance threshold offers a practical balance between reliability and maintaining system throughput..

5.4 Test case 2: Rotation offset estimation

In the case of rotational offset estimation, it was not feasible to implement a reliable method for physically measuring the actual rotation angle or the resulting positional deviation. This limitation stemmed primarily from the constraints of the experimental setup, which did not support precise angular measurements under controlled conditions. As a result, it was not possible to quantify the measurement error by directly comparing the estimated values to ground-truth rotation offsets.

To address this, a qualitative validation approach was adopted. Several rotational deviations were manually applied to the pallet, and the program's outputs were assessed visually. In all cases, the detected values exhibited a consistent and proportional trend relative to the applied rotation, indicating that the program performed as expected across varying rotational conditions.

Although no numerical error metrics were obtained for this test case, visual inspection confirmed that the estimated rotational offsets closely matched the manually introduced rotations in both direction and magnitude. It is worth noting that the rotation estimation function relies on both outer edge coordinates, specifically, the pairs (r_1, θ_1) and (r_2, θ_2), representing the radial distances and azimuth angles of the pallet's sides. However, only one of these pairs was validated in the horizontal offset tests. Despite this limitation, the consistent behaviour observed in practice, together with the shared geometric foundation between both estimation functions, suggests that the accuracy remains within acceptable bounds.

Since the calculated rotation results in a projected deviation along the y-direction (Δy), the same clearance constraint applies as in the horizontal offset scenario, namely, the estimated deviation must remain below the typical 50 mm clearance between the fork and the pallet tunnels to ensure safe operation. Therefore, assuming a similar error profile to that observed in the horizontal offset tests, the system is expected to provide adequate precision for operational use.

Nevertheless, future investigations should aim to validate the performance of the proposed solution through systematic and quantitative testing, ensuring a more rigorous scientific assessment.

5.5 Test case 3: Vertical offset estimation

This section aims to evaluate the proposed solution for estimating vertical offsets between the multiScan and the pallet. It begins by outlining the objective and the experimental setup used to perform the tests, followed by the presentation of the results and their corresponding analysis.

5.5.1 Objective and setup

The objective of this test case is to estimate the vertical offset and quantify the system's accuracy under controlled conditions. To this end, key performance metrics, namely the maximum absolute error and the mean absolute error, are calculated. These are then compared against the typical clearance between the SRM fork and the pallet tunnel to determine whether the estimated deviations remain within acceptable safety margins.

To apply controlled vertical offsets, objects of known thickness were placed under the multiScan sensor, thereby altering its height relative to the pallet. The thickness of each object was measured using a ruler. Figure 5.7 illustrates one such case, where an offset of 25 mm was introduced by placing stacked books totaling this thickness.

Throughout all measurements, the pallet remained in its reference position, with no horizontal offset or rotational deviation applied.

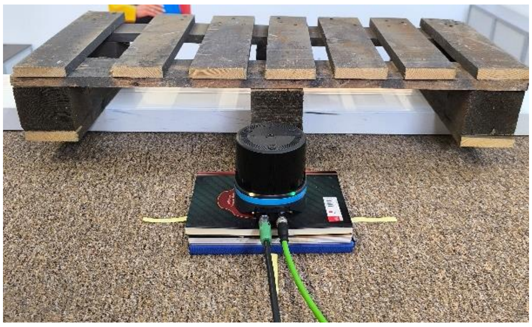

Figure 5.7 – Vertical offset of 25 mm induced by placing objects under the multiScan

5.5.2 Results and analysis

Table 5.2 presents the test results along with the corresponding errors and key performance metrics.

Table 5.2 - Results of the vertical offset estimation tests

Vertical offset estimation						
Test number	Real offset [mm]	Iteration	Measured offset [mm]	Absolute error [mm]	Maximum absolute error [mm]	Mean absolute error [mm]
1.	-15	1	-16	1	10	3
		2	-17	2		
		3	-17	2		
2.	-10	1	-13	3		
		2	-14	4		
		3	-20	10		
3.	0	1	0	0		
		2	0	0		
		3	0	0		
4.	5	1	6	1		
		2	5	0		
		3	4	1		
5.	10	1	14	4		
		2	14	4		
		3	15	5		
6.	20	1	26	6		
		2	26	6		
		3	27	7		
7.	25	1	29	4		
		2	29	4		
		3	30	5		
8.	30	1	34	4		
		2	35	5		
		3	34	4		

The results obtained for vertical offset estimation demonstrate a consistent performance across all test iterations, resulting in a maximum absolute error of 10 mm and a mean absolute error of 3 mm. As illustrated in Figure 3.13, the typical clearances between the SRM fork and the neighboring structure (pallet and beam) allow for a maximum permissible vertical offset of -10 mm downward and +20 mm upward. Any offset beyond these bounds would potentially compromising safe operation.

Given these constraints, and in light of the measurement errors observed, the tolerance threshold defined for fault detection must be set within a range that accounts for the system's maximum error. Specifically, it must lie above 0 mm and below +10 mm to ensure that any detected offset truly reflects a potentially unsafe condition. However, this introduces a number of limitations, particularly regarding the lower clearance bound.

In the case of negative vertical offsets, the absence of any safety margin (a range of measurement values that guarantee a safe diagnosis) presents a significant challenge. Since the lower bound of the tolerance threshold interval must be defined to 0 mm, any offset measured as negative must conservatively be classified as a fault to ensure safety. This implies that even real vertical deviations within the safe zone (for example, –5 mm) could be misclassified due to the error margin of up to 10 mm. As a result, all negative deviations detected by the system, even minor ones, will likely trigger fault flags, leading to a high rate of false positives and unnecessary interruptions to the SRM's operation.

For positive vertical offsets, the situation is slightly more favorable. With a maximum allowed deviation of +20 mm and a tolerance threshold set at 10 mm, there is a safety margin of 10 mm, which ensures that measured values between 0 and 10 mm guarantee safe operation. However, although the total clearance is 20 mm, applying a tolerance threshold of 10 mm (based on the maximum observed error) implies that real offsets between 0 and 10 mm may be overestimated. As a result, the system could interpret them as being within the 10 to 20 mm range, triggering a false fault detection. Therefore, even though a safety margin exists, false positives are still likely to occur which again limits the practical reliability of the proposed solution in this range.

In summary, although the system demonstrates acceptable precision for vertical offset estimation, its effective usability is constrained by the narrow tolerances imposed by the physical clearances, particularly in the negative direction, where no safety margin exists and errors lead directly to misclassification.

5.6 Test case 4: Structural fault detection

This section aims to evaluate the proposed solution for detecting structural faults in pallets using the multiScan's field evaluation function. It begins by outlining the objective and the experimental setup employed to carry out the tests, followed by the presentation and analysis of the results obtained.

5.6.1 Objective and setup

The primary objective of this test case was to verify whether the detection limits of the Field Evaluation function, as specified by the manufacturer, are consistent with real-world performance.

To conduct this assessment, four test objects with varying widths and heights were used. Each object was measured using a ruler, and its dimensions were recorded. For each object, three individual tests were carried out, placing the object inside the pallet tunnel at three different distances from the multiScan sensor. During each test, it was verified whether the system successfully detected the obstruction within the tunnel.

Figure 5.8 illustrates one of the test objects positioned within the pallet tunnel during testing.

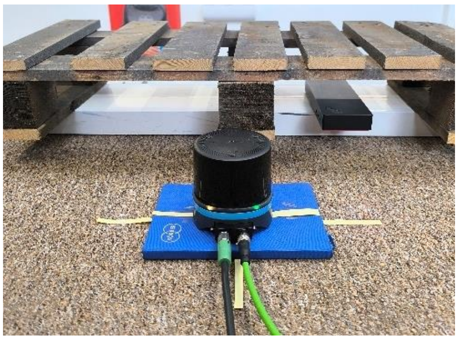

Figure 5.8 - Testing of Object 4 positioned within the pallet tunnel

5.6.2 Results and analysis

Table 5.3 presents the test results of structural fault detection.

Table 5.3 - Results of structural fault detection

Structural Fault Detection				
Object tested	**Distance to object [mm]**	**Width [mm]**	**Height [mm]**	**Detection result**
Object 1	150	10	55	FALSE
	250			FALSE
	350			FALSE
Object 2	150	23	60	TRUE
	250			TRUE
	350			TRUE
Object 3	150	195	18	TRUE
	250			FALSE
	350			FALSE
Object 4	150	90	30	TRUE
	250			TRUE
	350			TRUE

The test results demonstrate a strong alignment with the theoretical values provided in Table 3.2. It was observed that objects with a width of approximately 10 mm are difficult to detect, while from around 20 mm onwards, detection was consistently successful across all distances. Regarding object height, as expected, this dimension poses greater detection challenges for the multiScan due to its lower vertical resolution. Heights around 20 mm were detected only when the object was positioned close to the front face of the pallet (150 mm from the multiScan), but at distances beyond 250 mm, detection was no longer reliable. Object 4, with a height of 30 mm, was successfully detected at all tested distances.

The results confirm that thin objects become increasingly difficult to detect as the distance from the multiScan increases. Objects with dimensions near 10 mm were virtually undetectable at any distance. Widths of around 20 mm were reliably detected up to at least 350 mm, whereas heights of the same magnitude were not.

Finally, it is important to reiterate the limitation associated with the multiScan's shadow zone, which prevents it from scanning the full depth of the pallet tunnels. This issue was not directly tested, as the test pallet used had a tunnel depth of only approximately 300 mm.

5.7 Comparison of program execution times on S7-1200 and S7-1500 PLCs

Table 5.4 presents a comparison of the total program execution time measured on two different PLCs: the Siemens S7-1200 and S7-1500. The results show a significant performance difference, with the S7-1500 executing the same logic approximately ten times faster than the S7-1200 (0.3 s vs. 3 s).

Table 5.4 - Program execution time comparison between PLCs

PLC	Program execution time [s]
S7-1200	3
S7-1500	0.3

Additionally, Figure 5.9 illustrates the cycle time statistics obtained using the TIA Portal's online diagnostic and monitoring tools. The longest cycle times observed during execution clearly reflect the performance gap: 82.000 ms for the S7-1200 and only 9.310 ms for the S7-1500. In the case of the S7-1200, such long cycle times may compromise real-time performance, which is essential in industrial environments with strict timing requirements.

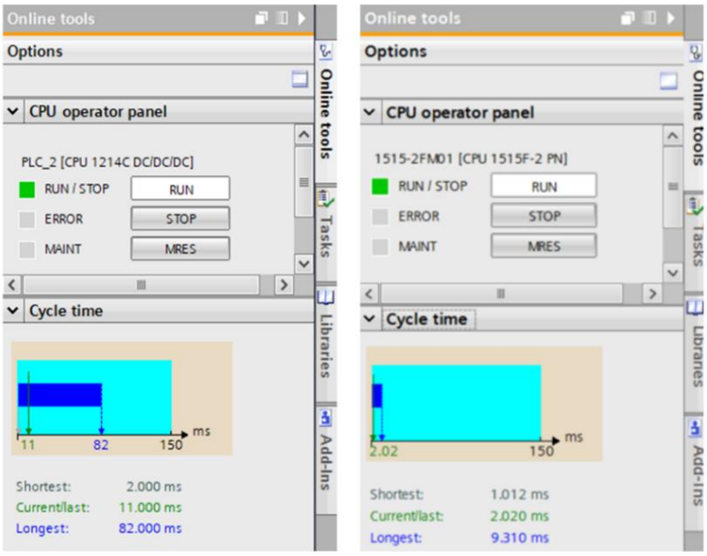

Figure 5.9 - Comparison of cycle times: S7-1200 (left) vs. S7-1500 (right)

These results demonstrate that, with the S7-1500, belonging to the same series as the PLCs used in the SRMs, the program can be further optimized to process larger volumes of data. This opens the possibility of increasing the horizontal resolution or using additional vertical layers to enhance the reliability and accuracy of feature estimation.

5.8 Global discussion of results

The errors observed in the tests arise from several factors, many of which could not be quantified or fully accounted for. One of the primary sources of error relates to the imprecision in fixing the system components in a defined, stable position. For example, no system was employed to ensure the multiScan remained in the exact same position throughout testing, which likely introduced some variability. Additionally, the method used to measure the applied offsets was not as precise as could have been achieved, contributing further to potential measurement errors.

Another important factor that may have influenced the measurement error is the resolution used in the program. Specifically, the 1-degree angular resolution may have a noticeable impact, especially at small angles, such as the azimuth angle (θ), where the laser beam intersects the pallet edges. This angle typically ranges between 18° and 25°. A difference of just 1 degree in this range leads to a significant change in the projection along the *y*-axis, i.e., the horizontal direction. As a result, the point cloud density decreases on the periphery of the angle, which can cause notable errors when estimating horizontal offsets or rotations. This phenomenon highlights the importance of using higher resolution in future tests, such as the 0.5° resolution offered by the multiScan165, to enhance accuracy.

Despite these challenges, several conclusions can be made with confidence. The functions for estimating horizontal offsets and rotations proved to be the most promising. The horizontal offset estimation, in particular, demonstrated good precision, especially considering the typical mechanical clearances of the real system. These two functions stand out as the most relevant for future investigations, as further testing is needed to assess their viability in a real-world SRM application.

In contrast, the vertical offset estimation and structural fault detection functions exhibited notable limitations. The former struggles primarily due to the tight mechanical tolerances of the system, which demand a LiDAR or other technology with greater precision. In the case of structural fault detection, several factors hinder performance, including the shadow zone of the LiDAR and its low resolution, which prevents the detection of anomalies below certain sizes. Among all the functions, this one performs the least effectively, but it still holds value in validating other functions by ensuring that there are no obstructions in the path of the SRM fork due to misalignment of the pallet, at least in the frontal plane.

Overall, the results can be considered satisfactory and promising, justifying further experimental campaigns. However, future tests should be carried out under more controlled conditions, with improved accuracy in displacement measurement and fixed mounting of all system components to minimize positional uncertainty.

Another avenue for future work would be to test the algorithm with alternative LiDAR sensors offering higher resolution and precision, especially given that the S7-1500 PLC demonstrated a strong ability to handle significantly larger data volumes. This observation reinforces the feasibility of scaling the system up by incorporating higher-density point clouds, which would further improve feature estimation accuracy.

Lastly, it is also important to recognize that the practical viability of this solution depends strongly on the layout and constraints of each specific warehouse or SRM. For example, pallet widths of 1000 mm or setups where the sensor is positioned very close to the pallet significantly reduce the system's ability to detect geometric features reliably, due to reduced scanning coverage and beam angle range.

Table 5.5 provides a synthesis of the main conclusions regarding the results of the four test cases.

Table 5.5 - Synthesis of Results and Conclusions

Test case	Conclusion
Horizontal offset estimation	Viable solution
Rotation offset estimation	Requires further investigation
Vertical offset estimation	Requires a device offering improved resolution and accuracy
Structural fault detection	Case dependent

5.9 Summary

Chapter 5 presented the experimental tests conducted to validate the proposed solution, along with the setup used for testing. The methodology for each test case was outlined, followed by the presentation and analysis of the results. The test cases focused on estimating horizontal, rotational, and vertical offsets, as well as detecting structural faults in the pallet. Key findings were discussed, including the comparison of execution times between two different PLCs. The chapter concludes with a global discussion of the results and insights into the system's performance and potential improvements for future investigations.

6 Conclusion

6.1 Review of the conducted work

This dissertation presented the development of a LiDAR-based solution for improving the safety and reliability of SRMs in automated warehouse environments. The project began with a detailed analysis of the problem, including the identification of operational vulnerabilities related to pallet misalignments and structural faults. Based on this, a set of technical requirements was defined, taking into account the integration constraints with the SRM system.

Following the conceptual phase, an in-depth study of the SICK multiScan165 LiDAR sensor was conducted to understand its characteristics, operating principles, and communication protocols. Particular attention was given to the structure and content of the data telegrams transmitted by the sensor, with the goal of enabling effective integration into the proposed solution.

Subsequently, the algorithms responsible for estimating the pallet's position and structural integrity were developed, along with the corresponding data model that supports these estimations. These algorithms were designed to interpret spatial information and identify positional offsets - horizontal, vertical, and rotational - as well as potential structural faults.

The next phase involved the integration of the multiScan165 sensor with a Siemens S7-1200 PLC. This included establishing reliable communication between the devices and implementing the full PLC logic required to receive, decode, and process the sensor data in real time.

Finally, a series of experimental tests was carried out to evaluate the performance of the developed solution. These tests were conducted in an experimental environment and served to validate the accuracy of the implemented solution, providing insight into the strengths and limitations of the proposed approach.

6.2 Challenges and achievements

One of the most significant challenges encountered during this project was the need to process high-volume 3D LiDAR data directly within a PLC environment. Unlike traditional programming platforms such as Python or MATLAB, where extensive libraries and optimized functions are available for point cloud and image processing, PLCs offer limited resources and low-level handling capabilities for managing such complex data structures. This constraint imposed a substantial programming effort, requiring the development of custom logic to interpret and manipulate raw sensor data efficiently.

Particular care had to be taken to ensure the program's computational efficiency, as excessive execution time would render the solution impractical for industrial deployment. In a real-time automation context, especially when integrated into critical systems like SRMs, execution time and determinism are essential. Achieving acceptable performance required careful memory management and optimized data extraction routines.

Despite these technical limitations, the project successfully resulted in the development and experimental validation of a functional and efficient solution. A complete program was created, and when tested with the S7-1500 PLC (established as the control unit for the SRM), it demonstrated the ability to estimate pallet positional offsets with errors below 10 mm. Notably, the algorithm achieves execution times of less than one second, demonstrating that real-time pallet evaluation based on 3D LiDAR data is technically feasible within the computational constraints of industrial PLCs. These results confirm the potential of the proposed approach for future integration in automated warehouse systems, where reliability and processing speed are critical.

6.3 Overall conclusions and future work

This study presented the development of a solution for estimating pallet features using the SICK multiScan165 sensor integrated with a Siemens PLC. Despite challenges such as inherent sensor inaccuracies and limitations in the experimental setup, the functions for horizontal offset and rotation estimation yielded promising results with satisfactory precision. In particular, horizontal offset estimation demonstrated significant potential for industrial application.

However, vertical offset estimation and structural fault detection revealed notable limitations, mainly due to mechanical tolerances in the system and the sensor's limited vertical resolution. While structural fault detection did not produce fully reliable outputs, it still contributed relevant indications regarding pallet misalignment.

The results underscore the need for further testing under more controlled conditions, with enhancements to the experimental setup and the use of higher-resolution LiDAR sensors. Future work should also focus on deploying the proposed solution in a real-world SRM operating within an industrial warehouse. This will allow for evaluating the system's performance in a dynamic and complex environment, accounting for variations in pallet sizes, warehouse layouts, and sensor positioning. Testing in such a context is essential to assess the robustness, scalability, and industrial applicability of the solution.

In conclusion, while the proposed solution shows promise, further improvements in sensor technology, calibration, and testing in operational warehouse conditions are needed to ensure its viability and effectiveness in industrial environments.

6.4 Personal assessment

From the author's personal perspective, the project proved to be both a significant and valuable challenge. Throughout its development, numerous technical difficulties and unexpected problems had to be addressed. Given that several of the technological concepts involved were unfamiliar at the outset, it was necessary to adopt a proactive and fast-learning attitude. The project demanded strong problem-solving skills and a high level of adaptability, which contributed substantially to personal and professional growth.

In particular, the experience allowed the author to further develop skills in PLC programming and industrial automation, an area of strong personal interest. It also provided the opportunity to engage with LiDAR technology, a modern and evolving field with growing relevance across multiple industries. Although many of the concepts encountered were new, the project aligned well with the objectives of the Automation master's programme. Having a solid foundation in this field proved to be highly beneficial throughout the course of the work.

References

1. "We are Körber". Körber. [Online]. Available: https://www.koerber.com/en/we/we-are-koerber. Accessed: Jun. 20, 2025.

2. O. F. Odeyinka, O. G. Omoegun, "Warehouse Operations: An Examination of Traditional and Automated Approaches in Supply Chain Management," in *Operations Management - Recent Advances and New Perspectives*, IntechOpen, 2023. doi: 10.5772/intechopen.113147.

3. "EPAL Pallets", Nedpal BV. [Online]. Available: https://www.nedpal.nl/index.php?item=product&id=1. Accessed: Jun. 25, 2025.

4. Körber Supply Chain PT, *Solutions for Pallet Handling and Storage: Technical Data Catalog*, internal document, 2021.

5. Körber Supply Chain PT, *RN5 – Arquitectura de Controlo dos Transelevadores (SRMs)*, internal document, 2023

6. Körber Supply Chain PT, *Sistema de Verificação de ULs*, internal document, 2023.

7. J. Ma et al., "A review of ToF-based LiDAR," *Journal of Semiconductors*, vol. 45, no. 10, p. 101201, Oct. 2024, doi: 10.1088/1674-4926/24040015.

8. H. Weber, *LiDAR Sensor Functionality and Variants*, white paper, SICK AG, 2018, 8022040.

9. T. Yang et al., "3D ToF LiDAR in Mobile Robotics: A Review," Feb. 22, 2022, arXiv: arXiv:2202.11025. doi: 10.48550/arXiv.2202.11025.

10. T. Regado, *Study and Optimization of the Control and Communication Architecture of a Rail Guided Vehicle System*, Master's thesis, School of Engineering, University of Minho, M.Sc. in Industrial Electronics and Computer Engineering, 2024.

11. SICK AG, *MULS1AA-114322 multiScan165*, product data sheet, Jun. 12, 2025. Available: https://www.sick.com/media/pdf/8/98/898/dataSheet_MULS1AA-114322-multiScan165_1147803_en.pdf.

12. SICK AG, *multiScan165*, operating instructions, 8028981/1P4M, Nov. 15, 2024. Available: https://cdn.sickcn.com/media/docs/3/73/273/operating_instructions_multiscan165_en_im0110273.pdf

13. SICK AG, *Data format description: Compact format and MSGPACK format for transmitting measurement data*, technical information, 8028133/1KK1, Jul. 20, 2023. Available: https://cdn.sickcn.com/media/docs/3/23/623/technical_information_data_format_description_en_im0104623.pdf

14. Siemens AG, "Product overview for SIMATIC S7-1200," *Siemens*. [Online]. Available: https://www.siemens.com/overview-simatic-s7-1200. Accessed: Jun. 26, 2025

15. "6ES7214-1AG31-0XB0". Siemens Industry Mall. [Online]. Available: https://mall.industry.siemens.com/mall/pt/pt/Catalog/Product/6ES7214-1AG31-0XB0. Accessed: Jun. 26, 2025.

16. Siemens AG, *SIMATIC S7-1200 Programmable Controller*, system manual, A5E02486680-AP, version 4.6, Nov. 2022. [Online]. Available: https://cache.industry.siemens.com/dl/files/829/109814829/att_1120874/v1/s71200_system_manual_en-US_en-US.pdf

17. SICK AG, *Telegram Listing: Ranging sensors LMS1xx, (...) multiScan*, technical information, 8014631/1PIK, Feb. 21, 2023. Available: https://www.sick.com/media/docs/7/27/927/telegram_listing_telegram_listing_ranging_sensors_lms1xx_lms5xx_tim2xx_tim5xx_tim7xx_lms1000_mrs1000_mrs6000_nav310_ld_oem15xx_ld_lrs36xx_lms4000_lrs4000_multiscan100_picoscan100_en_im0045927.pdf

All web pages were available at the dissertation's submission date (28/06/2025).